

1-1-2006

## Qualifications of duct rumble noise test system

Joshua Kading  
*Iowa State University*

Follow this and additional works at: <https://lib.dr.iastate.edu/rtd>

---

### Recommended Citation

Kading, Joshua, "Qualifications of duct rumble noise test system" (2006). *Retrospective Theses and Dissertations*. 19307.

<https://lib.dr.iastate.edu/rtd/19307>

This Thesis is brought to you for free and open access by the Iowa State University Capstones, Theses and Dissertations at Iowa State University Digital Repository. It has been accepted for inclusion in Retrospective Theses and Dissertations by an authorized administrator of Iowa State University Digital Repository. For more information, please contact [digirep@iastate.edu](mailto:digirep@iastate.edu).

# **Qualifications of duct rumble noise test system**

by

**Joshua Kading**

A thesis submitted to the graduate faculty  
in partial fulfillment of the requirements for the degree of

**MASTER OF SCIENCE**

Major: Mechanical Engineering

Program of Study Committee:  
Adin Mann, Co-major Professor  
Michael Pate, Co-major Professor  
Fredrick Haan

Iowa State University  
Ames, Iowa  
2006

Graduate College  
Iowa State University

This is to certify that the masters' thesis of

Joshua Kading

has met thesis requirements of Iowa State University

Signatures have been redacted for privacy

## Table of Contents

List of Figures .....	v
List of Tables .....	vi
Abstract .....	vii
Chapter 1 Introduction .....	1
1.3 Thesis Outline .....	4
1.4 Supporting Literature and Background.....	5
Chapter 2 System Description .....	8
2.1 Airflow System .....	8
2.1.1 Duct work.....	8
2.1.2 Fan Discharge Configurations .....	16
2.1.3 Outlet Plenum .....	21
2.1.4 Selection of Operating Conditions.....	23
2.1.5 Changes from the RFP .....	27
2.1.6 Acoustic Isolation .....	28
2.2 Measurement Systems .....	30
2.2.1 Sound level Tests .....	31
2.2.2 Airflow Measurement and Estimation.....	36
2.2.3 Pressure Drop Measurement.....	38
2.2.4 Fan and Motor Vibration Measurements .....	41
2.2.5 Additional Measurements .....	47
2.3 Method of Test.....	47
2.3.1 System operating points.....	48
2.3.2 Sound Pressure Level Tests .....	51
Chapter 3 Results: System Verification.....	54
3.1 Operating Point Verification.....	54
3.1.1 Airflow rate Repeatability.....	55
3.2 Sound Measurement Repeatability .....	55
3.2.1 Repeatability of sound level measurement at a point .....	57
3.2.2 Repeatability of the Room Sound Level.....	59
3.3 Vibration and Balancing .....	62
3.3.1 Peak Velocities.....	62
3.3.2 Vibration Effect on Sound .....	65
3.4 System Modes.....	69
3.4.1 Room Modes.....	69
3.4.2 Duct Modes.....	72

Chapter 4 Preliminary Sound Results .....	75
4.1 Baseline Sound level.....	75
4.2 Configuration Change.....	76
4.3 Narrow Band Data .....	80
4.4 Difference of Operating Points .....	83
4.5 Velocity Profiles .....	84
Chapter 5 Summary and Conclusions.....	87
5.1 Summary.....	87
5.2 Conclusions.....	89
5.3 Recommendations for Future Study .....	91
References.....	96
Appendix Twin City Fan Information .....	97

## List of Figures

Figure 1.1 ASHRAE Outlet conditions .....	1
Figure 2.3 Inlet Volume Damper to the Fan room.....	12
Figure 2.4 Enclosure around transition duct work.....	14
Figure 2.5 Four fan outlet configurations. ....	18
Figure 2.6 Schematic of the Mounting Base for the fan and motor assembly.....	20
Figure 2.7 Support Base the mounting base rests on the middle bar.....	21
Figure 2.8 Outlet Plenum diagram.....	23
Figure 2.9 Fan Curve provided by Twin City Fan Company .....	24
Figure 2.10 Measured Noise Reduction between the fan and measurement room.....	29
Figure 2.11 Transition enclosure with MDF covering the inlet to the system .....	30
Figure 2.12 Floor microphone locations.....	33
Figure 2.13 Microphone locations on joints A and B.....	34
Figure 2.14 Microphone, plastic sleeve assembly .....	35
Figure 2.15 Pressure Traverse locations .....	37
Figure 2.16 Location of the pressure drop measurement.....	39
Figure 2.17 Accelerometer Axes .....	42
Figure 2.18 Mounting Location of Tri Axial Accelerometer on the Motor.....	43
Figure 2.19 Mounting location of Tri Axial Accelerometer on the Fan.....	43
Figure 2.20 Magnitude of the velocity time signals recorded by data acquisition. ....	45
Figure 2.21 Velocity Frequency Spectra of the fan and motor.....	46
Figure 2.22 Operating points set points along the fan curve. ....	49
Figure 2.23 Example of setting operating points.....	51
Figure 2.24 The Order of the measurements. ....	52
Figure 3.1 Repeatability of the 35% WOF at 2.5 inch pressure drop.....	60
Figure 3.2 Repeatability of the eight operating conditions of the fan .....	61
Figure 3.3 Velocity Peaks.....	63
Figure 3.4 Peak Velocities of each operating point .....	64
Figure 3.5 Peak Velocities at the operating conditions.....	65
Figure 3.6 Average discrete frequency spectra.....	66
Figure 3.7 Spectrum Vibrations of the Fan.....	67
Figure 3.8 Fan Cage Supports.....	69
Figure 3.9 Average Discrete Frequency Spectra in the Measurement Room.....	71
Figure 3.10 Sound level distribution chart.....	72
Figure 3.11 Average Discrete Frequency Spectra in the Duct.....	73
Figure 4.1 Average one-third octave band sound levels.....	77
Figure 4.2 Sound Level Differences .....	78
Figure 4.4 Narrow Band Sound Level Data.....	81
Figure 4.5 Narrow Band Sound level data of configuration 1 and configuration 4. ....	82
Figure 4.6 Room Sound levels difference in (dB). ....	84
Figure 4.7 Power output difference of the VFD (hp).....	85
Figure 4.8 Velocity profile of configuration 1 and configuration 2 .....	86
Figure 4.9 Velocity profile of configuration 3 and configuration 4 .....	86

## List of Tables

Table 2.1 Fan Curve Values.....	25
Table 2.2 Calculated Values for Operating Points.....	26
Table 2.3 Measured Operating Points of the Baseline Configuration .....	50
Table 3.3 Flow rate repeatability. ....	55
Table 3.1 The measurement repeatability from 16 through 250 one third octave bands..	58
Table 3.2 Repeatability of Sound Measurements (dB).....	62
Table 3.4 Operating Points, Fan Speed Frequency and Peak frequencies.....	68
Table 3.5 Predicted Modes in the Measurement Room.....	70
Table 3.6 Duct Mode Predictions .....	73

## Abstract

*Duct rumble noise is commonly attributed to the poor aerodynamic discharge conditions of fan outlets. Thus far, qualitative descriptors have been used as guidelines for engineers to limit the amount of duct rumble noise. The objective of this study was to create and verify a test facility that would accurately quantify the amount of duct rumble noise that was caused by the change in discharge conditions of a fan and duct system. Valid data will then be used to replace the qualitative descriptor with quantitative predictions. A key design constraint of the testing system is that it can the change in sound due to the fan discharge configuration.*

*The test facility was capable of changing between fourteen different discharge conditions. There were four different fan orientations: a fan in front blast condition blowing directly into the duct work, a fan in upblast, with rotation towards the elbow, a fan upblast rotating with the elbow, and a fan upblast rotating against the elbow. Each of these was measured with the fan outlet at different distances away from the duct inlet. The “optimum” or frontblast had two distances between the fan and inlet, the rest of the orientations had four distances between the fan and the inlet. The fan was operated at eight operating points on the fan curve to accurately measure the effect of changing configurations on rumble noise. The duct and measurement system was designed to easily measure and verify the sound pressure level effect of the fan discharge conditions.*

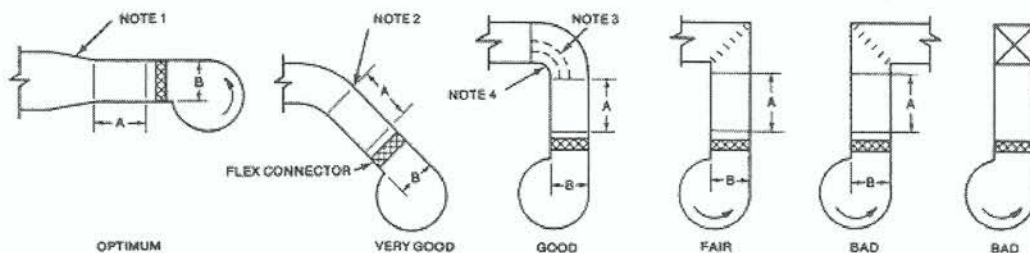
*The sound measurements were taken at one-third octave bands between 16 and 300 Hz. The narrow band analysis was taken up to 800 Hz. The measurements were taken in an acoustically isolated room at nine locations in the room and seven locations in the ductwork. The accuracy of the measurement was within  $\pm 1$ dB, which was far less than the 3 to 11 dB variations that are caused by the fan configuration.*

## Chapter 1 Introduction

### 1.1 Background

The discharge configuration of a fan can adversely affect the low frequency duct rumble noise downstream of the fan. Rumble noise, defined as noise in between the 16Hz and the 300 Hz octave bands, is considered by many practicing engineers as an indication of turbulence caused by poor fan discharge conditions.

In the 2003 ASHRAE (American Society of Heating Refrigeration and Air-conditioning Engineers) Applications Handbook, Chapter 46 figure 17 (Figure 1.1) is a qualitative diagram correlating the discharge configuration with a qualitative descriptor of the resulting noise. There is no sound level data that is connected with the qualitative descriptor. The descriptor does give a rough guideline, but it does not give a means to predict the increased rumble for various designs. The predictions are needed for good comparisons of design alternatives such as weighing the cost of modifying the orientation and position of the fan compared to noise control measures such as lagging or lining the duct. With noise level predictions, then the various design alternatives can be effectively compared.



NOTES: 1. SLOPES OF 1 IN 7 PREFERRED. SLOPES OF 1 IN 4 PERMITTED BELOW 2000 fpm (10 m/s).  
 2. DIMENSION "A" TO BE A MINIMUM OF 1.5 "B" WHERE "B" IS THE LARGEST DISCHARGE DUCT DIMENSION.  
 3. RUGGED TURNING VANES SHOULD EXTEND FULL RADIUS OF THE ELBOW.  
 4. MINIMUM OF 6 IN. (150 MM) RADIUS.

**Figure 1.1** ASHRAE Outlet conditions

The exact level of the relationship between duct rumble noise and aerodynamic disturbances has not been quantified to the knowledge of the researcher. There are no sound pressure level data to support the qualitative descriptors given in the ASHRAE Handbook and therefore, this leads to poorly designed outlet conditions for fans. The building design methods in the past ten years have been to use less space and lighter weight building structures, which means that higher aspect ratios are needed in ducting. All these factors make duct rumble noise more and more prominent. The best way to eliminate the duct rumble noise is at the source, and it has always been assumed that the source of duct rumble noise comes from the fan discharge conditions. However, there are many reasons that one may not be able to adhere to good aerodynamic design conditions.

The energy consumption of an HVAC (heating ventilation and air-conditioning) system also increases with poor discharge conditions, and this energy consumption can be directly related to the duct rumble. With limited space for fan fitting, the fan may discharge directly into the ductwork inlet, and this condition will cause an extra pressure drop on the system. In addition, to eliminate the rumble noise generated, plenums, duct lining and other noise control devices may be employed thus causing even further pressure drop on the system.

A system that can quantify the amount of duct rumble noise that is generated by the discharge conditions would be able to give good engineering guidelines for HVAC acoustics. Therefore, ASHRAE (American Society of Heating Refrigeration and Air-conditioning Engineers) funded a project to provide information on the changes in rumble noise generated by various fan configurations. In addition to providing predictions of the rumble noise

levels, an auxiliary goal of the work was to identify the mechanisms for the changing rumble noise.

## **1.2 Research Scope**

To measure the acoustic effects of aerodynamic disturbances at a fan discharge, a test facility needed to be built and verified to produce reliable data. The fan and motor assembly had to be able to meet four of the ASHRAE configurations that are shown in Figure 1.1. The assembly also had to be able to achieve different distances away from the inlet to the test duct work. The fan had to be able to run at multiple speeds and at multiple operating loads. In order to achieve the different discharge conditions, the fan must be mounted such that it can be rotated to achieve up-blast and front-blast orientations. The fan and motor base must be able to rotate to achieve the perpendicular orientation. To meet the requirement of distances between the fan and the elbow, the duct work needed to be able to be removed and replaced. The structure of the fan and motor assembly had to be able to raise and lower according to the ASHRAE requirements, and still be rigid enough to handle the stress. The fan had to run at multiple speeds and thus needed to be controlled by a variable speed drive. The fan also had to run at multiple load curves so a volume damper needed to be installed in the system.

The measurements that needed to be made are sound levels within the room and within the duct. Volume flow rate and fan pressure drop measurements needed to be taken to verify the operating conditions of the fan. The variables in the system that can be controlled were the fan speed and the inlet restriction. The measured variables when setting the operating conditions were the airflow rate, the pressure drop and the brake horse power.

The sound level measurements needed to be taken with attention being paid to low frequencies. The measurement room had to be acoustically isolated from the rest of the system with a noise reduction of at least 13 dB. This isolation was done to ensure that it was noise coming from the duct that was being measured. Sound level measurements were taken in multiple locations throughout the room in all three dimensions in order to give an overall sound level of the room. The multiple points were also used to analyze specific room modes. Likewise, sound measurements were taken in the duct to check for duct modes.

### **1.3 Thesis Outline**

The complete test system that was created will be described in Chapter 2. The system needed to consist of a ducting system for the airflow that can be modified to accommodate the multiple test conditions. It also will describe the fan and motor base, and how the assembly can be moved. This section also covers the inlet and outlet of the system, and how the system properties are controlled to obtain an operating point. The room that the measurements were performed in required isolation; the process to isolate will be discussed. Chapter 2 also covers the various measurements that the test system records. Such as the sound levels measurements, the vibration measurements of the fan and motor assembly, the pressure drop measurements and the airflow measurements of the fan. The methodology of taking all of these measurements is covered in the method of test section of chapter 2.

There are two results chapters. The first is the system verification, chapter 3. This chapter covers the reliability of the data. The repeatability of the sound data is critical to use it in comparison with other sound levels. The repeatability of the room measurements must be lower than the changes in sound level that are being compare or else the data recorded is

meaningless. The purpose of this study is to test and analyze the effect of aerodynamic disturbances on the duct rumble not the effect of vibrations on duct rumble. To be sure that this is what is being measured the vibration of the fan and motor assembly was analyzed in Chapter 3 to verify what the system was measuring. The possibility of modes in a room and in the duct could adversely affect the sound levels that are recorded. For this reason the room and duct modes were analyzed and made sure that they did not impact the sound levels.

The second results chapter covers the data that was acquired and some preliminary analysis of that data. It is recommended by the ASHRAE committee that the data be compared to a “baseline” measurement at the optimal condition. Chapter 4 will go into detail on how this baseline is set and how it is used. The sound levels at each configuration seem to show trends. The comparison between the configurations is shown in Chapter 4. The difference between configurations at specific operating points also may be a useful way of looking at the data, and is included in this chapter. The velocity distribution does not include sound data but this does give insight to what is happening in the duct, therefore it is presented in Chapter 4.

## ***1.4 Supporting Literature and Background***

Because the research was focused to provide data that is not available in the literature, a detailed literature review of rumble noise was not performed. Instead, the literature review focused on issues related to the design of the complete testing system.

The test system was defined in the ASHRAE RFP (request for proposal). The duct work, fan model, the configurations that were required and the fan operating points that the system was going to run at, were predefined in the RFP. References were given to ASHRAE

and AMCA (Air Movement Control Association) standards to give guidelines about the design and building of the duct. The number of sound measurements was also defined in the RFP.

ASHRAE Fundamentals Handbook (2005) had a lot of needed information on designing the system, such as: duct design standards, measurement standards, and aerodynamic estimations. The ASHRAE Fundamentals Handbook (2005) gives the relationship for a rectangular duct to achieve similar flow properties as a round duct of the same effective duct diameter. One of the methods that have been used is to nondimensionalize the distance used in varying the distance from the fan to the duct. In order to nondimensionalize the distance, it was expressed in terms of the distance in between the fan and duct inlet ( $L$ ) over the effective duct diameter ( $D$ ). As stated before, the aerodynamic effects on a system are assumed to have the highest effect on the duct rumble. The ASHRAE Fundamentals Handbook gives an estimation process to limit the turbulence at the exit of a fan system. The ASHRAE Fundamentals Handbook also gives standards on how to arrange a pressure traverse that is used to measure the airflow rate across a rectangular duct. The ASHRAE Fundamentals Handbook is also used to estimate the pressure losses over sections of the duct that cannot be measured.

ASHRAE Systems and Equipment Handbook (2004) was used to determine the operating conditions by using standard fan laws as trusted values. ASHRAE Applications Handbook (2003) gave the fan discharge conditions in qualitative descriptors of the duct rumble, instead of the aerodynamics of the system. The ASHRAE Applications Handbook also covered the paths that sound could travel into the measurement room. ASHRAE Laboratory Standards 51-1999 gave methods for measuring the pressure drop across a fan.

These standards also included the AMCA standard for the arrangement of the motor and fan base.

Bies and Hanson (2002) was used for sound pressure level standards. The sound level averages over nine points in the measurement room and seven points in the duct. Bies and Hanson (2002) had a trusted method for averaging the room sound levels in terms of octave bands and narrow band frequencies. Bies and Hanson also discussed the mode identification for rooms and ducts.

## Chapter 2 System Description

The system is divided into an airflow system, a measurement system, and a method of test. In addition to the ductwork, the airflow system includes the fan discharge conditions, fan and motor mounting system, and the inlet and outlet conditions. The measurement system consists of sound, airflow and vibration measurements. Finally, the method of test for collecting the data pays particular attention to the selection and tuning of the operating conditions. Each of these system elements will be discussed.

### **2.1 Airflow System**

The airflow system consists of many parts including the duct work, the inlet throttle, the fan conditions (and the process by which they are changed), the outlet plenum, and the operating conditions of the fan. The duct work consists of a volume damper, fixed duct section and a variable duct section.

#### **2.1.1 Duct work**

The facility consists of three rooms shown in Figures 2.1 and 2.2: a fan room, a measurement room and an outlet room. The fan room is the inlet to the duct system. The inlet to the fan room is controlled with a hole in the door. The area of the hole can be increased or decreased, thus acting as the volume damper to the duct system. The fan room is 13'-7" x 10'-1" and 10'-8" tall where the measurement room is also 13'-7" x 10'-1" and 10'-8" tall. These are the desired room dimensions to limit the number of low frequency room modes in the measurement room and to simulate an office environment. Both the fan

room and the measurement room have structural insulation walls, as well as insulated floors. Further, the ceiling is not connected to the rest of the building.

## **Volume Damper**

The volume damper, shown in figure 2.3 controls the amount of air that inlets to the system. The volume damper is one of the controlled variables of the system. After a meeting with one of the ASHRAE committee members (Schaffer 2004), it was decided to have the inlet of the system be the volume damper. The door to the fan room is used as the volume damper. The initial design for the inlet to the system was to have the door be converted to an inlet plenum, and have the volume damper at the outlet of the system. The inlet plenum was designed to control noise into the system; however it was restrictive to the airflow intake. The inlet plenum was removed, and it was determined it was not needed to control the noise of the system.

A 72 inch by 24 inch hole was cut in the center of the fan room door that is 2 foot- 10 inches wide by 6 foot 10 inches tall. The hole is then blocked off to regulate the airflow. There is a sliding sheet of medium density fiberboard that is 3 foot 2 inches tall by 2 foot 2 inches wide. This board slides between two metal track guides, pins hold the MDF sheet in place while the fan is running. The board gives analog control over a portion of the damper. The rest of the control comes from three notches that block the bottom half of the door. These notches can be removed to allow for more airflow or placed back on the door to restrict airflow. Two of the notches have 11 inch heights and the bottom notch has 12 inch height.

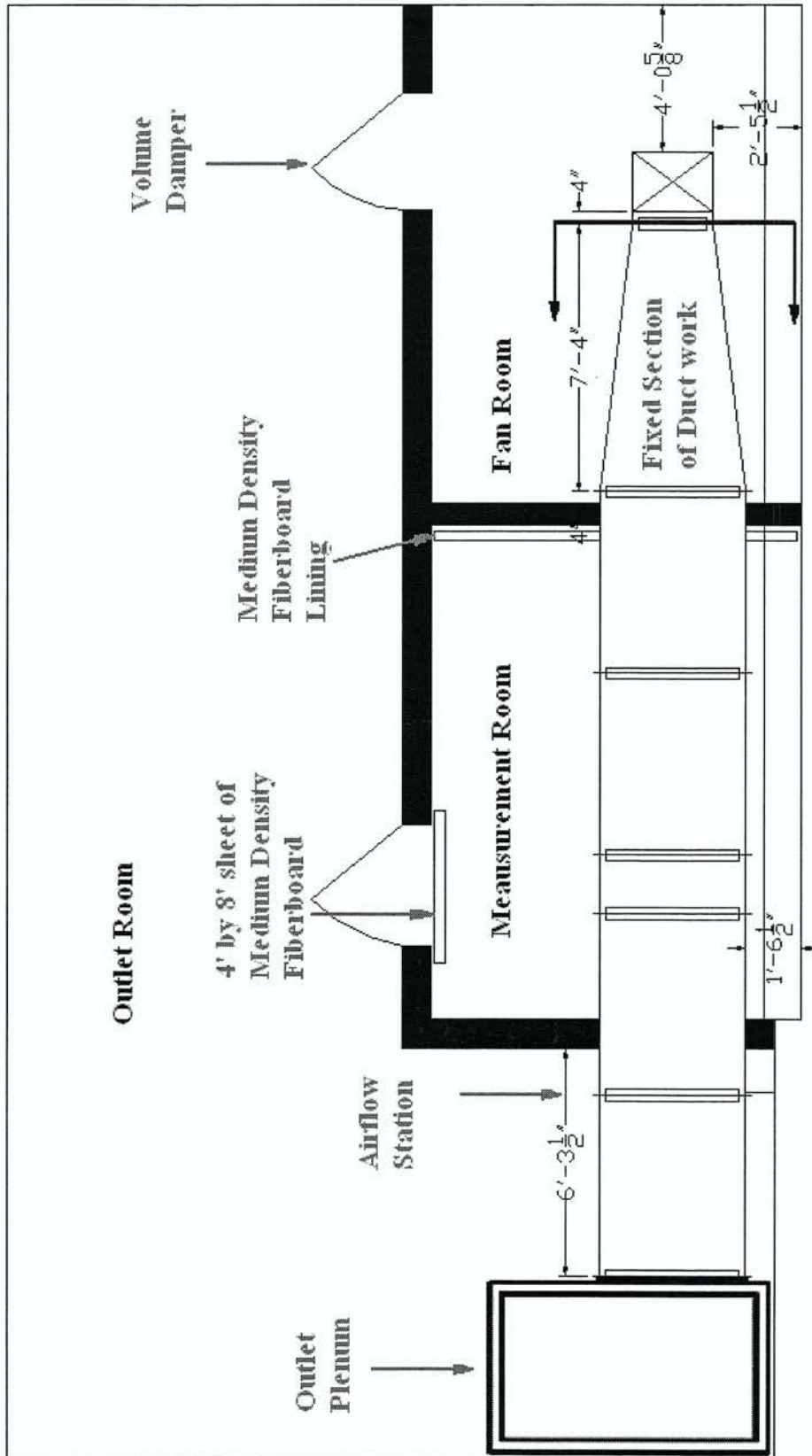


**Figure 2.1** Room Layout, there is an inlet restriction on the door of the fan room. The measurement room is acoustically isolated from the rest of the system. The outlet room is open to the rest of the building.

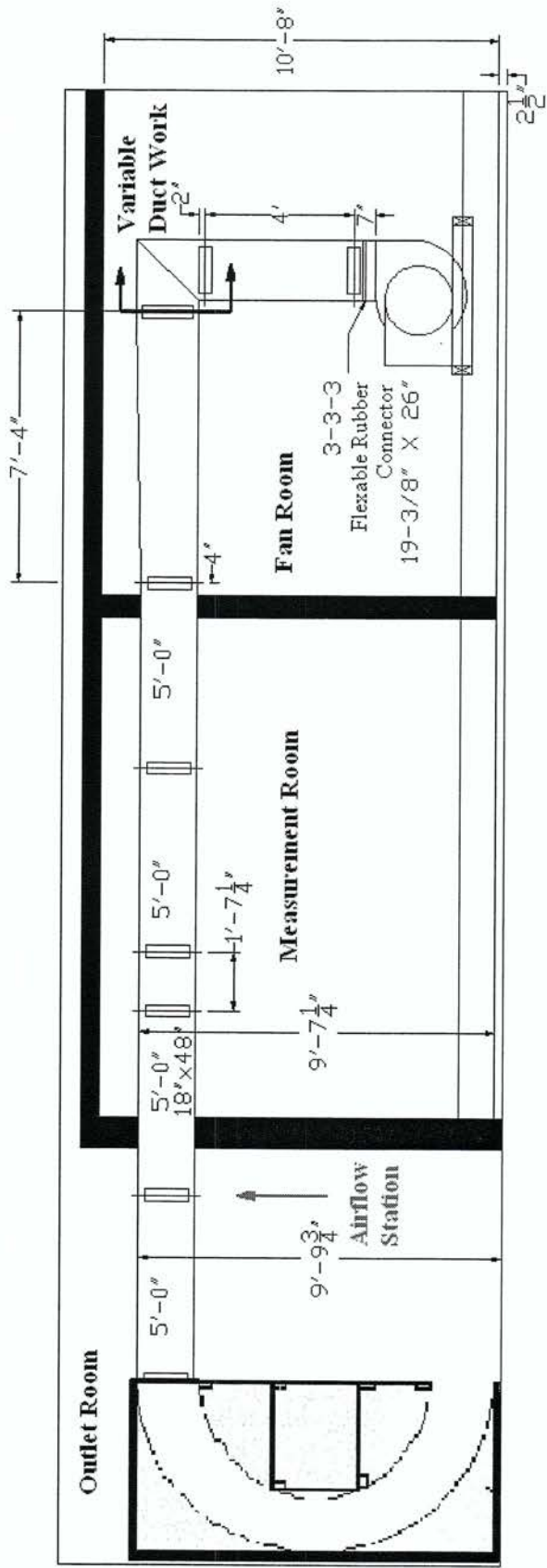
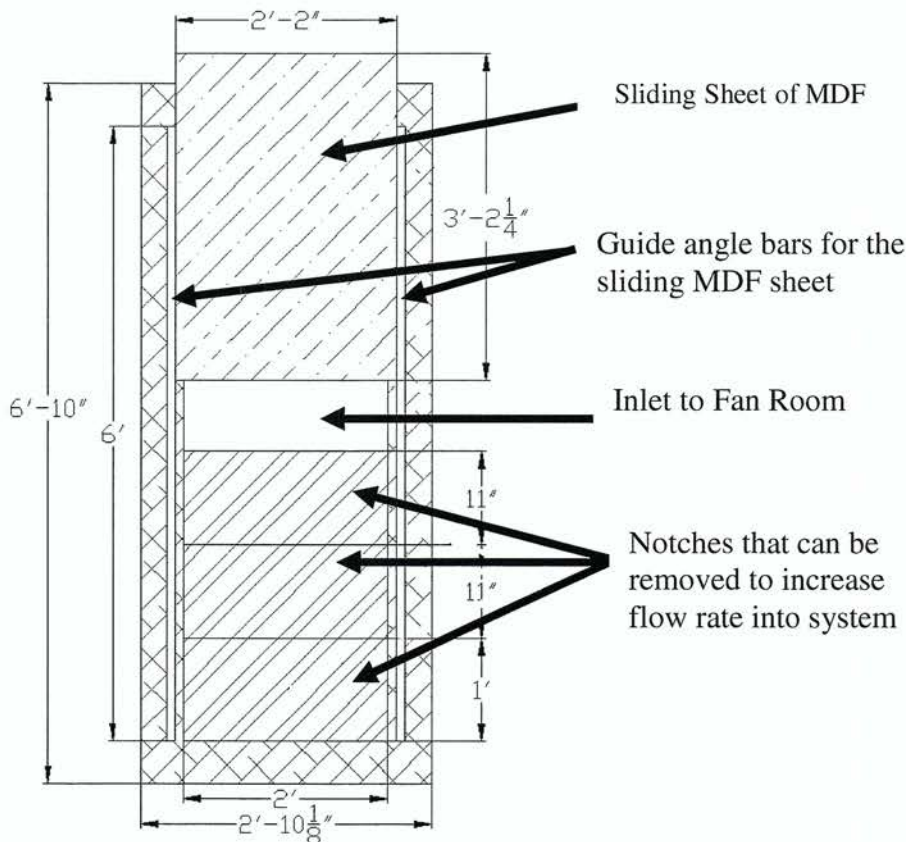


Figure 2.2 Room Layout Side View.

The reason the notches have different heights is because at high flow rates the effect of volume flow rate is relatively insensitive to the area change. Thus when the bottom notch is removed, there is no need for complete analog control over the inlet as there is when the first or second notch is removed. The top notch and the sliding sheet of MDF can be overlapped thereby completely shutting off the air intake.



**Figure 2.3** Inlet Volume Damper to the Fan room

The fan can experience a great amount of imbalance if the airflow into the system is not even. For configurations one through three, one of the inlet sides to the fan is open to the door. The other inlet to the fan is on the opposite side away from the door. This means that most of the air will enter directly into one side of the fan as opposed to traveling around it to enter the opposite side. For this reason, in addition to the volume damper, there is a sheet of

¾” plywood that is placed in front of the inlet to the fan. The plywood is affixed to the support base. It acts as a baffle and breaks the direct airflow path to the inlet of the fan. The plywood must be at least 18 inches away from the inlet and preferably as far away from the inlet as the wall on the opposite side of the fan. The baffle is needed in any of the configurations where the fan is lower than the top of the inlet damper. Therefore, the baffle is only needed in configurations two and three when the fan is either at two duct diameters away from the elbow or if the fan and motor assembly is on the ground. The baffle is not needed when the fan is above the volume damper inlet because there is no direct path the airflow must first travel into the room and then up.

### **Fixed Duct Work**

The duct work is made from 22 gage sheet metal, and is installed with no insulation lining. Each joint is constructed with easily modified j-ward duct mate. The constant section of the duct work begins at a transition piece that extends from the middle of the fan room to the fan room wall. This transitions the outlet of the fan 19.4 inches x 26.0 inches to the measurement section of the duct which is 18 inches x 48 inches. The transition has a length of 7 foot - 4 inches, which gives a slope ratio of 1:4. ASHRAE Applications (2003) recommend a slope of 1:7 to 1:4.

The transition is enclosed in a 53 inches by 93 inches by 3 foot tall box constructed from MDF (medium density fiberboard) and lined with 2 foot by 4 foot sheets of 2 inches duct board fiberglass as shown in Figure 2.4. The box was designed to isolate the transition duct from break in noise from the fan room. The ceiling is lined with three layers of the duct board fiberglass, the bottom of the MDF enclosure is lined with two layers of the duct board

fiberglass, and the sides are lined with one layer of the duct board fiberglass. To limit the amount of duct wall vibration damping that the enclosure causes, the fiberglass duct board is suspended at least  $\frac{1}{2}$  inches away from the duct work. The fiberglass is suspended by wire that is padded with cardboard so it does not tear the fiberglass and hung from the ceiling.

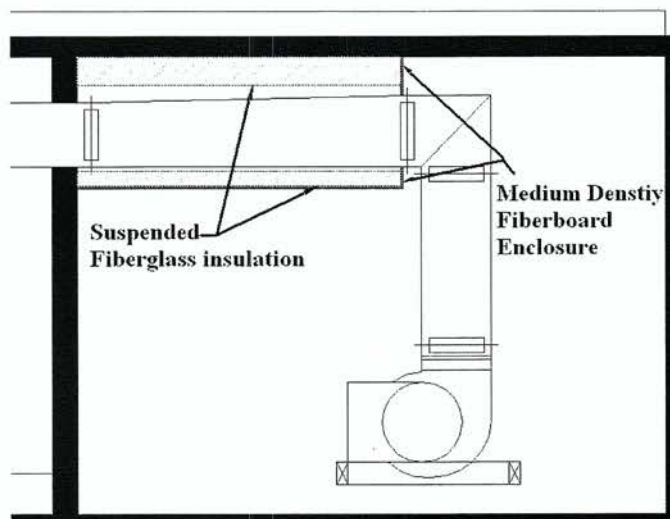
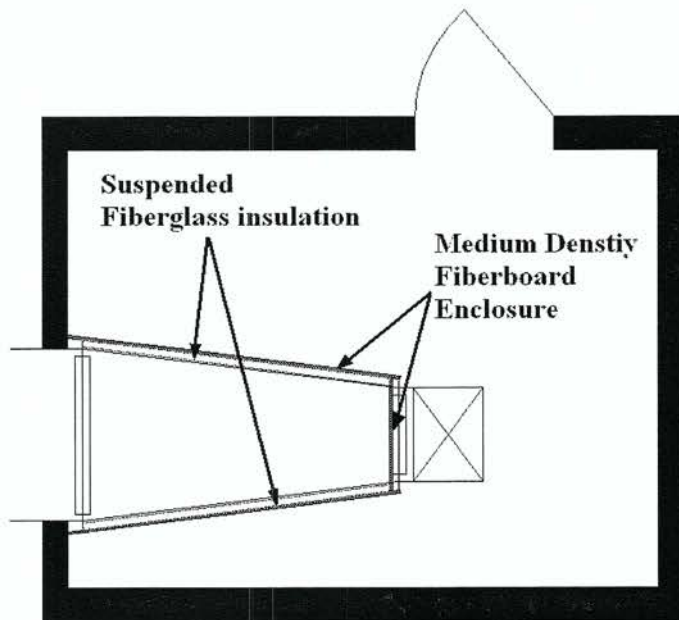


**Figure 2.4** Enclosure around transition duct work

The duct work continues through the measurement room and out into the outlet room. This section is 21 feet – 7 inches long and terminates into an outlet plenum designed to keep noise from the outlet room back into the measurement room. The outlet plenum will be described in more detail later in this chapter.

The ducting is 5 foot sections with stiffening creases every 12 inches and a 1-1/2 inch angle support bars every 2 feet -6 inches running along the exterior of the 48 inches length of the cross section. In the measurement room, there is a single section that is in fact 1 foot -7 inches. This was done to make the duct as long as possible. The joint is in the measurement room because of installing issues, so that a 5 foot section could be used to exit the wall of the measurement room. On all the joints of the constant section of the duct work, there are j-ward clamps, as well as bolts that join the duct together. In the joints of the constant section, a sealing adhesive was applied.

### **Variable Duct Work**

The inlet to the duct system can be varied depending on the desired fan configuration. The fan always has a flexible rubber connector at the outlet; this is a 3 inch – 3 inch -3 inch (3 inches of fan flange, 3 inches of rubber flex, and 3 inches of duct flange) flexible duct connector. The fan can discharge directly into the duct system or (as shown in Figure 2.2) the fan can discharge into a length of duct and then into an elbow. In Figure 2.2, the fan is shown in an up blast position, with a straight length of duct 48 inches long, and then the elbow at the inlet to the fixed section of ducting.

When the elbow is not in place the farthest distance between the fan and the transition can be extended is 24 inches away. In most of the configurations, there is a 90° elbow into the transition piece. The distance between the fan and the elbow can be up to 55 inches long. The duct work from the fan to the elbow is the same dimensions as the fan outlet. The elbow inlet and outlet dimensions are equal to the fan flange (19.4 inches by 26 inches). The elbow has 11 double wide turning veins spaced evenly apart. The fan can be moved up or down with a supporting base that will be described in the fan discharge configurations section.

The duct is still the same dimensions as the fan outlet, and it can be up to 55 inches long. The last piece of duct work that can be added to the system for the duct configuration is a short transition piece. The piece inlet is 26 inches by 19.4 inches and the outlet is 19.4 inches by 26 inches, while the length is only 7 inches. This transition piece allows for the fan to be rotated 90° to take measurements. On all of the joints in this section of the duct the ducting is bolted together, j-ward clamps are used when possible and duct tape was applied to the exterior of the ducting joints.

### **2.1.2 Fan Discharge Configurations**

To measure the effect the fan discharge condition has on the duct rumble noise downstream of the fan, the test system needed to be flexible enough to achieve each of the discharge conditions, a total of fourteen discharge conditions. There are four fan configurations, in Figure 2.5, three of which can have four different lengths between the fan and the duct system inlet, and one that can have two different lengths between the fan and the duct inlet. The distance between the fan and the elbow will be measured in terms of an

effective duct diameter, the diameter of an equivalent round duct. The effective duct diameter is given by ASHRAE Fundamentals (2005)

$$D_h = 1.3 \frac{(H \times W)^{0.625}}{(H + W)^{0.25}} \quad 2-1$$

where H and W are the height and width, respectively. The effective duct diameter for the fan outlet used in this research is 24 inches. The distance from the fan outlet to either the elbow or transition duct, D in Figure 2.5, will be measured in terms of the effective duct diameter for the fan outlet. There are 4 distances away from the elbow that are achieved by the system 0, 1 (24 inches), 2 (48 inches) and 2.3 (55 inches) duct diameters. The distance between the fan outlet and the first flow disturbance can have a great impact on the aerodynamics of the system.

The ASHRAE Fundamentals handbook (2005) gives a recommendation on duct design, and the distance  $L_e$  that the fan should be from flow disturbances,

$$L_e = \frac{V_0 A_0^{0.5}}{10,600}, \text{ for } V_0 > 2500 \text{ fpm} \quad 2-2$$

$$L_e = \frac{A_0^{0.5}}{4.3}, \text{ for } V_0 \leq 2500 \text{ fpm} \quad 2-3$$

This length  $L_e$  depends on size of the duct and airflow speed. The faster the flow then the more turbulent and the more distance is needed for the flow to become fully developed. However, these distances are rarely put into practice. Since this study requires us to run the fan at a single configuration and at multiple speeds, it is not possible to put this calculation into practice. The distances are instead measured in effective duct diameters.

The specification on the design of the test system is that four different fan discharge conditions could be tested with four different lengths of duct from the fan to the first

transition in the system. The measurements were to be performed at 8 operating points of the fan, to be accomplished by varying inlet restriction to the fan and the fan speed. The design and verification of the test system along with initial results are presented.

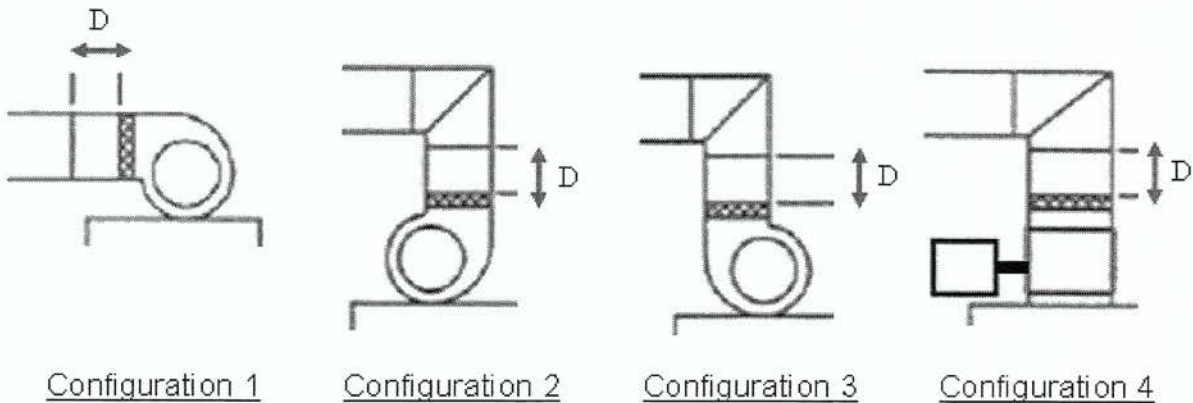


**Figure 2.5** Four fan outlet configurations. The distance  $D$  is the length that can be varied from 0 to 1 in configuration 1, 0 to 2.3 in configurations 2, 3 and 4.

Configuration 1: The fan is in front blast orientation and blows directly in to the transition duct. Because of limitations in the fan room dimensions the fan could only be moved 1 duct diameter from the transition piece.

Configuration 2: The fan blows the air into the elbow that allows the air moved to follow a natural curve. This configuration can be moved 0 to 2.3 duct diameters away.

Configuration 3: The fan blows against the natural curve of the elbow. Configuration 3 can be moved 0 to 2.3 duct diameters away from the elbow.

Configuration 4: The fan blows perpendicular to the duct. In this configuration there is a transition piece at the elbow that directs the air into the duct system. The transition piece is 7" long, and therefore the fan must always be at least 7" away from the elbow. For

configuration 4, this is considered to be the 0 duct diameters away from the elbow. The fan can then be moved 1, 2 and 2.3 duct diameters away from the elbow.

## **Mounting Base**

In order to measure all of these configurations, the fan must be capable of rotating on two axes. The fan must also be mounted in such a way that it can be lifted up and down depending on the distance to be measured. To do this, the fan is always mounted to a “mounting base” (Figure 2.6). The mounting base is a double steel strut that holds the fan and motor assemble together. The mounting base has six isolation springs that it rests on. The four corner springs are Amber Booth type XL, Style C, 800 lb, 1inch isolation springs the middle two are Amber Booth type XL, Style C, 300 lb, 1inch isolation spring. For configuration 1, the motor needs to be raised to reach the keyway of the fan shaft. This is done by adding two additional cross beams directly under the motor.

## **Support Base**

The mounting base is supported by the support base (Figure 2.7). The support base is also made of Flex Strut FS-201, 1-5/8” 12 gage 2x combination channel, and kept up by six pillar supports of Flex Strut FS-201, 1-5/8” 12 gauge. The top and bottom cross bars are to help support. The structure the middle bars can be shifted up or down depending on the configuration or duct diameter that is desired. The isolation springs from the mounting base rest directly on the middle bar of the support structure. Additional diagonal beams are added on the sides and across the center to give extra rigidity and support. Because of the changes in the structure, the diagonal beams are not in the same location between configurations.

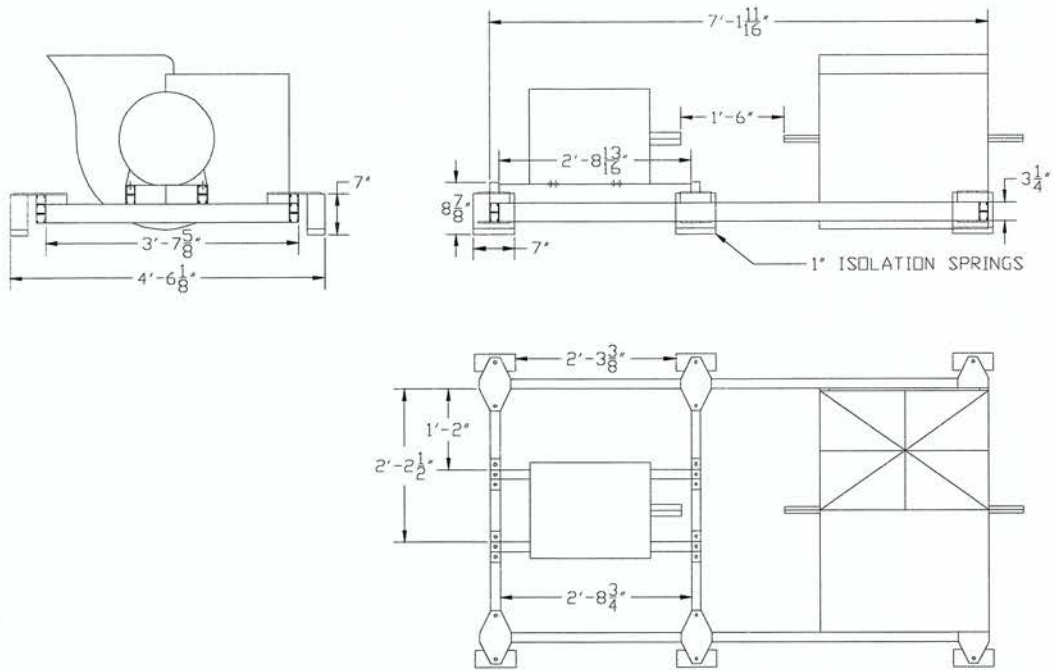


**Figure 2.6** Schematic of the Mounting Base for the fan and motor assembly with the fan in the up blast discharge position.

The fan and motor are mounted to a structural base according to ASHRAE arrangement 8 with a direct drive shaft. The motor, a Baldor EM 2532T-25 hP motor, is controlled with a Baldor Series 15 Inverter control variable speed drive. The motor speed can be varied up to the peak speed of 1194 rpm. The motor and fan are connected with a Rexnord 18" coupler model PT46F. The coupler was chosen such that the assembly could handle a slight amount of flex. The fan is a Twin City Fan Company NFC; size 182 Class 2, double wide/double inlet, forward curve 18-inch diameter wheel, scroll fan.

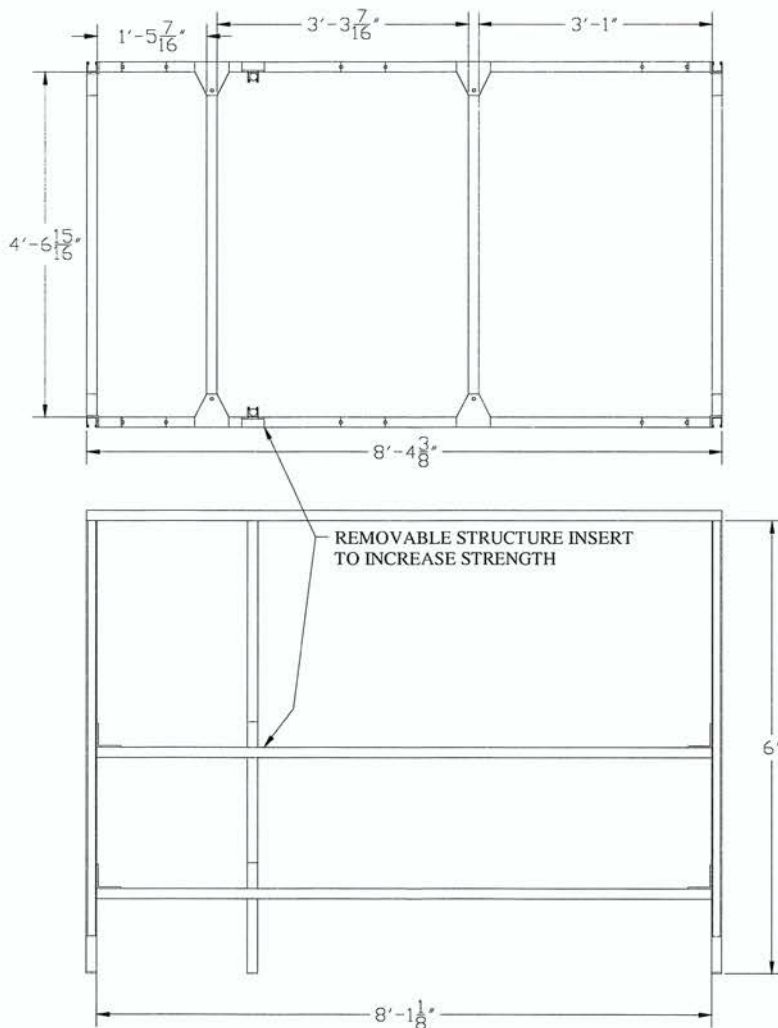


**Figure 2.7** Support Base the mounting base rests on the middle bar. More cross beams and diagonal beams are added for support.

### 2.1.3 Outlet Plenum

The air flow exits into an outlet plenum that is constructed as a sound trap to keep any excess noise from traveling from the outlet room back into the system (Figure 2.8). The outlet plenum has an internal path that forms an arc from the duct at the top of the plenum to the outlet at the bottom of the plenum. The exterior is made from medium density fiber board shell that is mounted on a 2x4 structure. The interior consists of three layers. The first is

fiberglass board 2 foot by 4 foot by 2 inch, and these boards were cut to be stacked and fill in between the MDF and the duct lining insulation. The second layer is duct board fiberglass that is 1 inch by 48 inch by 120 inch sections. This lining is the section that the air is directly against and is designed to withstand high velocities. The last layer is perforated metal that is used to create a rigid lining to the insulation. The perforated metal is aluminum sheet metal oval pattern with a width of .032 inch, 20 gage, that held in place by wire hangers and stapled to the exterior walls (where possible) at the inlet and exit. The curve of the internal path is kept at a radius of 42 inches. The inlet to the plenum is the same as the duct (18 inches by 48 inches); the air flow is sloped to an exit of width of 5 foot -4 inches. The slope is only on one side as the other side is obstructed by a wall.

At an ASHRAE Technical Committee meeting, it was decided that the air velocity at the exit would be too high and needed to be controlled. If the velocity is too high the outlet turbulence might cause turbulence and noise upstream in the system. It was required that only turbulence from the fan was measured thus the outlet was increased to a width of 5 foot-4 inches. This gives a  $\frac{3}{4}$  inlet to exit ratio in order to control the air velocity and the turbulence that is generated at the exit.

The initial design of the outlet plenum was intended to be against the wall of the measurement room and discharge the air away from the wall. The interior of the plenum would be a system of baffles that would keep noise from flowing back into the system. After a meeting with ASHRAE Technical Committee member Mark Schaffer it was decided that the design would cause unneeded pressure drop at the outlet. Moving the plenum farther away from the wall enabled more duct length, and a section for the airflow station.

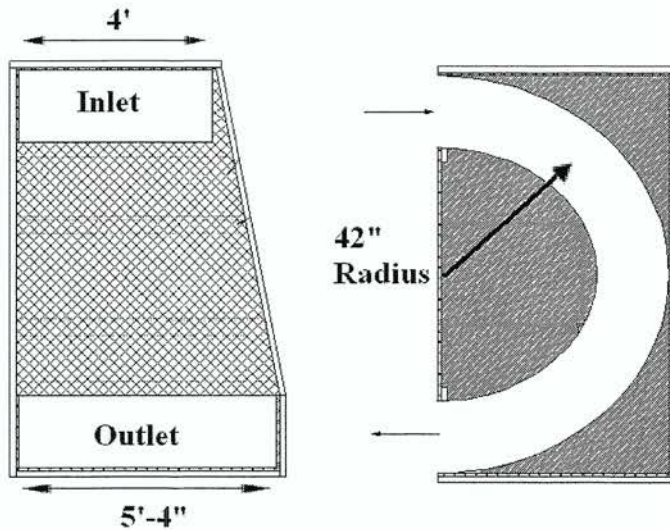


**Figure 2.8** Outlet Plenum diagram, the inlet is screwed to the outlet of the system duct.

#### 2.1.4 Selection of Operating Conditions

The operating points that the fan needs to be run at were stated in the RFP. These populate the fan curve, and should give a representation of the effect on sound level at different settings on the fan curve. This fan curve, Figure 2.9, is used as a basis for setting all of the operating points. The eight required operating conditions are:

- One fan speed at 1.0 inch of water pressure drop that represents the 90% wide open flow load curve.
- Two fan speeds at 1.0 and 2.5 inches of water pressure drop that represents the 80% wide open flow load curve.
- Three fan speeds at 1.0, 2.5 and 4.0 inches of water pressure drop that represents the 60% wide open flow load curve.
- Two fan speeds at 2.5 and 4.0 inches of water pressure drop that represents the 35% wide open flow load curve.

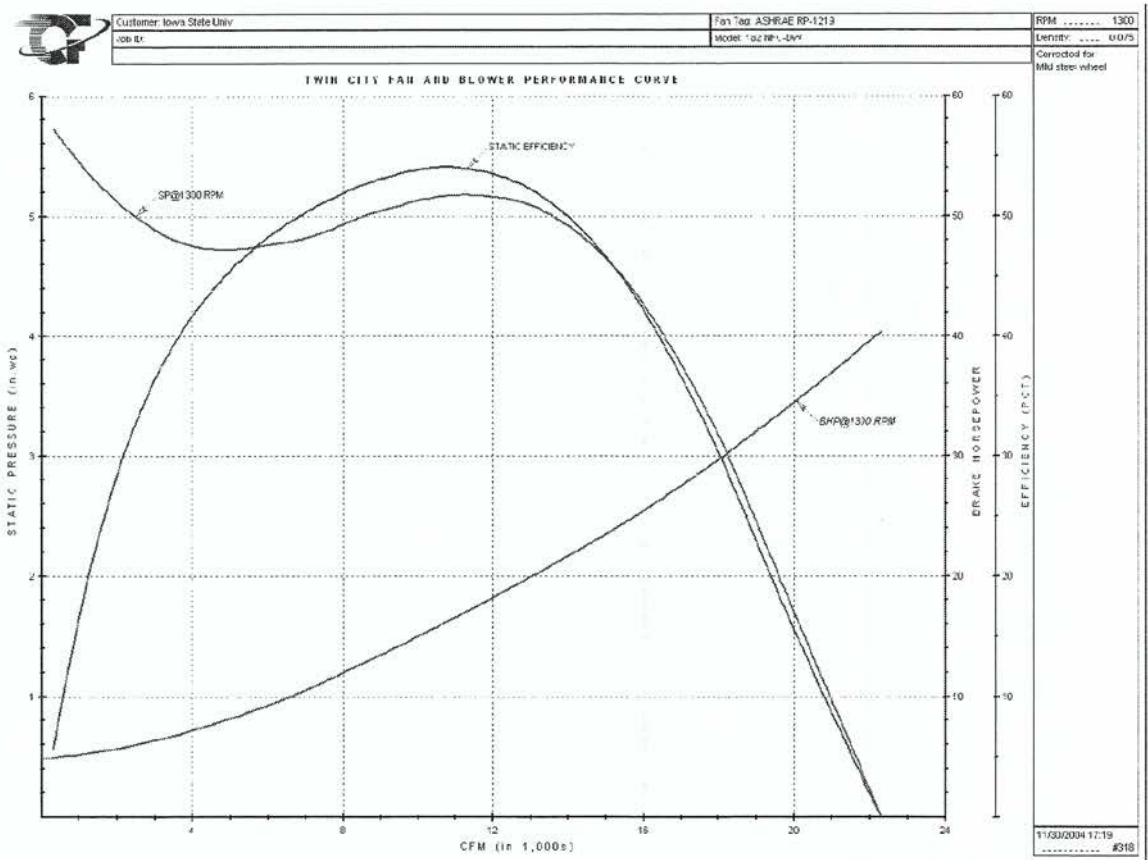


**Figure 2.9** Fan Curve provided by Twin City Fan Company

To set the operating condition, there are two measured quantities and two controlled variables. The pressure drop and the volume flow rate are the measured variables, and the inlet restriction and fan speed are the controlled variables. The operating points had to be set in a way that the two variables could be controlled by the fan speed and the inlet restriction. The fan speed can be set and the inlet restriction can be varied until the desired airflow rate is achieved.

To set the operating conditions, the desired airflow rate and the desired fan speed needed to be calculated using the fan laws. The values in Table 2.1 are taken from Figure 2.9. These values are all at an rpm of 1300 varying from load. The load curve is referred to

the percent wide open flow (%WOF). The fan pressure curve at 1300 rpm reaches a maximum volume flow rate of 22,200 CFM, at 0 pressure drop in inches of water. A special test facility is required to get a 100% WOF curve at 0 pressure drop, however, it is still used to find the remaining values.

**Table 2.1** Fan Curve Values

% of Wide Open Flow (%WOF)	Volume Flow Rate (CFM)	Fan Pressure Drop (inches water)
100%	22,200	0
90%	19,980	.1.74
80%	17,760	3.33
60%	13,320	5.03
35%	7,770	4.9

ASHRAE Systems and Equipment (2004) give the fan laws for speed and airflow rate in terms of the pressure drop,

$$N_1 = N_2 \left( \frac{p_1}{p_2} \right)^{\frac{1}{2}} \quad 2-4$$

$$Q_1 = Q_2 \left( \frac{p_1}{p_2} \right)^{\frac{1}{2}} \quad 2-5$$

Where:

$N_1$  = the desired fan speed (rpm)

$N_2$  = 1300 rpm

$p_1$  = the desired pressure drop (inch wg)

$p_2$  = the pressure drop of the %WOF (inch wg)

$Q_1$  = the desired volume flow rate (CFM)

$Q_2$  = the desired volume flow rate of the desired %WOF (CFM)

These are applicable if no external changes are made to the fan, meaning if the %WOF stays the same. So, to obtain the desired fan speed of a %WOF, the known values for the pressure drop at 1300 RPM can be used in equation 2-4. Likewise, to obtain the

values for the desired airflow rate, the known values for pressure drop and volume flow rate at 1300 RPM can be used in equation 2-5.

Table 2.2 has the calculated values of the fan speed and the volume flow rate in terms of the set values of %WOF and fan pressure drop. In Table 2-2 the operating conditions defined by the ASHRAE committee are listed in the first two columns the second two columns are the calculated values found using the fan laws.

**Table 2.2** Calculated Values for Operating Points in Terms of %WOF and Pressure Drop

% of Wide Open Flow (%WOF)	Fan Pressure Drop (inches water)	Fan Speed (rpm)	Volume Flow Rate (CFM)
90%	1.00	986	15,147
80%	1.00	712	9,732
	2.50	1,126	15,388
60%	1.00	580	5,939
	2.50	916	9,391
	4.00	1,159	11,878
35%	2.50	929	5,550
	4.00	1,175	7,020

The conditions in Table 2.2 are the desired operating conditions. To set the operating conditions the first step is to set the system to a desired load curve. This is done by setting the fan at the speed of one of the operating points. The inlet restriction is then varied until the desired flow rate is obtained.

The other operating points are obtained by changing the fan speed to the required value. The flow rate is measured, but the inlet restriction is not varied to compensate for any difference between the measured and desired flow rate. Setting the operating points requires determining the setting of the inlet restriction for each of the load curves for each of the fan/duct configuration.

### 2.1.5 Changes from the RFP

It was necessary to make several changes from the RFP in order to conduct this project. The basic design is the same, however there are a number of restrictions that the room size put on the duct system.

The initial RFP calls for a transition slope of 7:1. This is based on the ASHRAE recommendations given in the ASHRAE Applications (2003). However, it was decided that 4:1 ratio is acceptable given that the 7:1 ratio would force the transition duct work to be 12'-10". The room itself is only 13'-7", and in order to have an elbow and duct system, the room was not large enough to accommodate the 7:1 ratio. This ratio is also not commonly used in practice. The 4:1 ratio was settled on to give a reasonable flow transition.

The RFP also calls for the constant duct to be 72" x 12". This would require the 4:1 transition to be 15'-4", which is greater than the length of the fan room. The decision was made by the committee to change the dimensions to 48" x 18" and 22 ducting gauge instead of 20 gage. This duct gauge was based on SMACNA standards. By doing this, the total cross sectional area remained the same and the effective stiffness remains similar. The 72" x 12" has an  $EI=0.00315 \text{ lbin}^2$ , and the 48" x 18" has an  $EI=0.00335 \text{ lbin}^2$  this is a 6% change.

There is also a call for a three duct diameter distance for the distance D in figure 2. This is rarely seen in practice and the duct height is limited by water lines that run in the outlet room. This requires the top of the 9'-9 3/4" from the floor of the outlet room. The insulation along the floor of the fan and measurement room lifts the fan up, which all cuts down on the largest distance the final measurement can be. It was decided that 55" would be a sufficient distance to determine the effect of the duct diameter.

On the “optimum” configuration, all 4 duct diameter lengths were to be tested, but again this exceeds the size of the fan room and redundant. Therefore, the 2 duct diameter and 3 duct diameter measurement of the “optimum” configuration was removed.

### **2.1.6 Acoustic Isolation**

The sound measurements were taken in the measurement room. It is critical that the measurement room be acoustically isolated from the rest of the system. Any noise in the room could contaminate the sound data. Sound could enter through many ways as shown in ASHRAE Applications (2003). There are no return or supply air vents in the room. So the major concerns are the airborne noise that is transmitted directly through the wall, the structural noise that is transmitted through the floor and walls (also known as flanking paths), and the breakout noise that is generated from the duct itself. Of these three, the only one that needed to be measured was the breakout noise of the duct. The other two paths had to be minimized so the measurements could reflect the change in noise of the duct.

ASHRAE required a transmission loss between the measurement room and fan room of at least 13 dB at one-third octave bands between 16 Hz and 250 Hz. The transmission loss was interpreted as noise reduction (Beis and Hanson, 2002) for this research. Noise reduction measurements were therefore performed in the rooms with the duct and outlet plenums installed. The inlet to the transition section was blocked off with a medium density fiberboard sheet. The noise reduction measurements were done by placing a broad band white noise source in the fan room and taking eight measurements in the fan room, and then taking nine measurements in the measurement room. The points were measured in dB and averaged using log<sub>10</sub> scale. Measurements were performed in the one-third octave bands

between 16 and 250Hz (Figure 2.10). The initial noise reduction measurements had very low noise reductions at two of the one-third octave bands, 16 and 50 Hz.

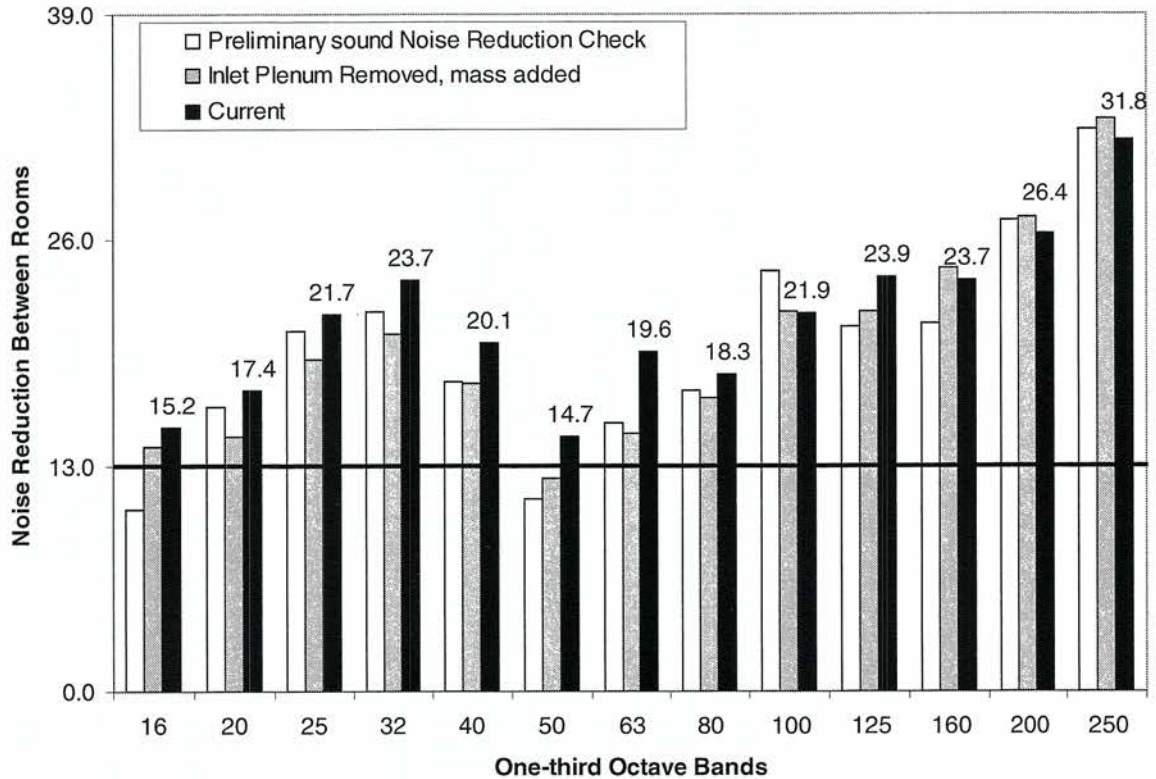


**Figure 2.10** Measured Noise Reduction between the fan and measurement room

The duct work was passed through holes in the walls that were  $\frac{1}{2}$ " to  $\frac{3}{4}$ " larger than the duct. Cracks and holes create airborne paths for sound transmission so these had to be sealed. The duct is framed around the wall openings with MDF leaving a small gap so as once again the MDF is not touching the duct work. Fiberglass insulation is added in the large gaps for absorption. The small holes into the room were stuffed with fiberglass and then covered with drywall plaster. Any remaining gaps around the duct or in the room were sealed with a silicon caulking. Absorption was added to the interior of the measurement

room by means of lining the walls with fiberglass insulation. The absorption had no effect on the noise reduction so the insulation was removed. The interior of the measurement room separating wall was lined with MDF for additional mass. Finally the door to the measurement room was discovered to be a transmission path. An inlet plenum was designed to keep sound from entering the system through the inlet. This plenum over restricted the airflow and had no effect on the noise in the system. The plenum was then removed. The duct work entrance was covered by a sheet of MDF that covered the inlet shown in Figure 2.11. The door inlet to the measurement room was covered by a sheet of MDF. This increased the noise reduction to above the desired levels.

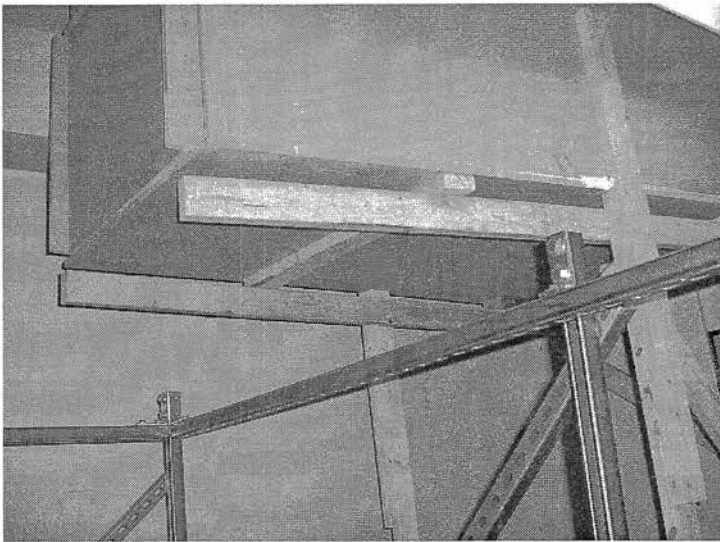


**Figure 2.11** Transition enclosure with MDF covering the inlet to the system

## ***2.2 Measurement Systems***

The measurement systems consist of the multiple tests that are conducted throughout the experiment: the sound pressure level tests, the pressure drop measurement and estimation, the airflow measurement and the vibration measurements. Each of these are needed to properly determine not only the effect of the aerodynamics on the system but also what

exactly is being measure, and the specific operating conditions of each. This section covers the operation of each of these measurement systems.

### **2.2.1 Sound level Tests**

The sound pressure level tests are the primary measurement of this study. The purpose of this study is to determine the effect that aerodynamic disturbances have on low frequency duct rumble noise. Duct rumble noise is defined as high sound levels in octave band at and below 250 Hz. The sound level tests take place in the measurement room and along the duct in the measurement room. The sound pressure level in the room and in the duct is measured in both narrow band frequency spectra and one-third octave band frequencies.

Sound measurements are taken with a Bruel & Kjeaar Pulse data acquisition system. The sound level measurement system allows the user to control the frequency range and number of lines in the spectra. These are varied by the user to obtain data over a sufficient frequency range and at the frequency resolution that is needed to identify significant features in the spectrum. The recorded frequencies in the narrow band are 0 to 1,000 Hz with 1600 lines, a frequency resolution of 0.63Hz, for the configuration 1 and no duct diameters. For the next case of configuration 1, 1 duct diameter before the duct system, the recorded frequencies were reduced to 0 to 800 Hz with 3200 lines, a frequency resolution of 0.16 Hz. For the remainder of the configurations the frequencies recorded are 0 to 800 Hz with 6400 lines, a resolution of 0.13 Hz. The recorded one-third octave bands data was acquired over 12.5 to 20,000 Hz. The results that are analyzed for this study are the one-third octave bands of 16 to 250 Hz. The sound pressure level is recorded by two ACO Pacific Inc. microphones

model # 4012, and input to an ACO Pacific Inc. acoustical interface model PS9200. The signal is then output to a Bruel & Kjaer Pulse data acquisition system type 3560C. This system has both a CPB analyzer that records the one-third octave band average over 30 seconds and a narrow band frequency analyzer that takes 100 averages. The amount of averaging that was needed was determined by how long it took to reach a constant mean. For both the one third octave band and the narrow band frequency, the amount of averaging was varied to determine how much was needed. Chapter 3 goes into further detail as to why 30 seconds was chosen as the averaging time for the one third octave band data.

The sound measurements consist of a microphone grid of 16 locations, 9 locations in the room and 7 in the duct. There are two reasons multiple locations were measured in the room. The first was that to get an overall sound level throughout the room. Every point in the room may have a different sound level, so all of these points must be averaged to get an overall sound of the room, a typical practice in room acoustics. The second reason was to identify room modes. The room geometry can cause a resonance in the sound levels, causing unusually high levels at a specific frequency. 7 locations in the duct are chosen for the same reasons; however, the overall sound level in the duct is less important. Identifying duct modes is the primary concern of the duct, since a duct mode could transfer power efficiently to the room. This will be discussed in greater detail in Chapter 3.

The 9 microphone room locations are spaced out in a 3 by 3 grid, shown in Figure 2.12, with the rows spaced 30 inches apart and columns spaced 40 inches apart. The array is spaced 30 inches from the building north wall and 36 inches from the building west wall. These measurements are staggered at different heights: 36 inches, 56 inches and 81 inches above the floor. Different measurement heights are used so the measurements represented a

spatial average of the sound and to reduce the potential for a single mode to dominate the response. The three levels are denoted as L1, L2 and L3 in Figure 2.12.

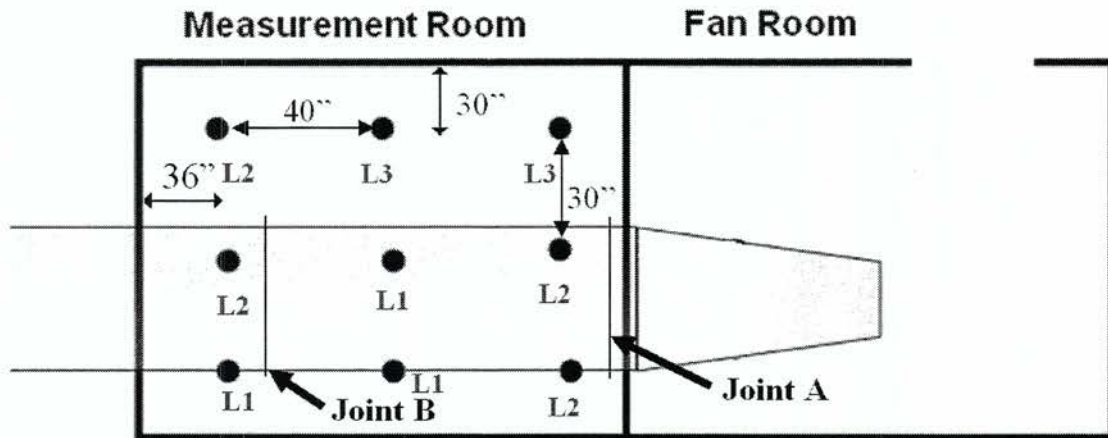


**Figure 2.12** Floor microphone locations.

The seven locations on the duct were distributed along two joints of the duct. The microphones were mounted near joints in the duct to minimize the stiffness changes created by the microphone mounts. Joint A in Figure 2.13 consisted of a single microphone location at the bottom corner of the duct. This joint is  $\frac{3}{4}$  inches after the duct enters the measurement room. Joint B in Figure 2.13, is 53 inches away from the outlet room wall. Six microphone mounts are located along this joint. Five of the microphone locations are along the bottom evenly spaced 12 inches apart; the sixth is along the side of the duct 9 inches above the duct.

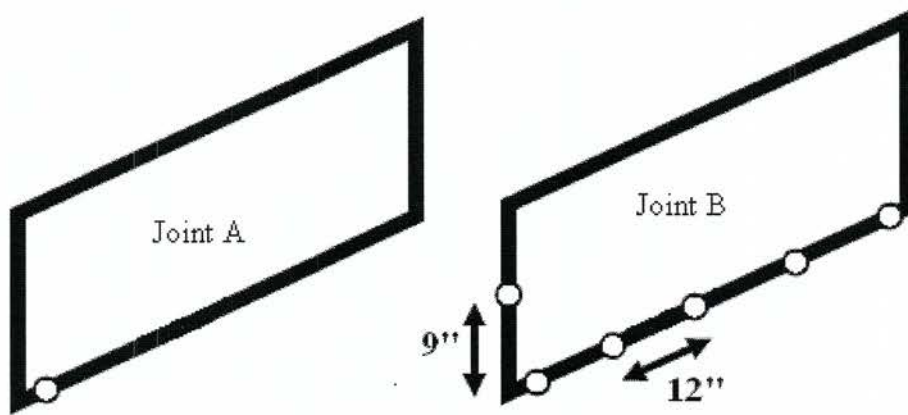


**Figure 2.13** Microphone locations on joints A and B

Each mount consisted of a plastic sleeve assembly, shown in Figure 2.14. The microphone was held with a rubber capped screw so as not to damage the microphone. The Plexiglas tube assembly consists of two sections. The top inch has an inside diameter of  $\frac{1}{2}$  inch the bottom 1 inch is  $\frac{9}{16}$  inch inside diameter. The microphone has an outside diameter of  $\frac{1}{2}$  inch and fits easily into the sleeve's bottom but protrudes into the sleeve's top. To keep the microphone in place, a screw was put through a threaded hole in the plastic against a rubber layer taped to the side of the microphone. The top 1 inch of the sleeve contains fiberglass so that the microphone is not in direct contact with the air flow in the duct. The sleeve assembly was positioned flush to the duct with a  $\frac{1}{2}$  inch diameter hole in the duct. The tube assemblies were mounted to all seven measurement locations in the duct. When a microphone was not inserted into one, a  $\frac{1}{2}$  inch diameter wood dowel was inserted to minimize sound transmission through the assembly. An O-ring was mounted on the microphone tip inside the holder to minimize airflow through the holder. The concepts for this holder design were based on similar designs used by a member of the ASHRAE Committee (Wise 2005).

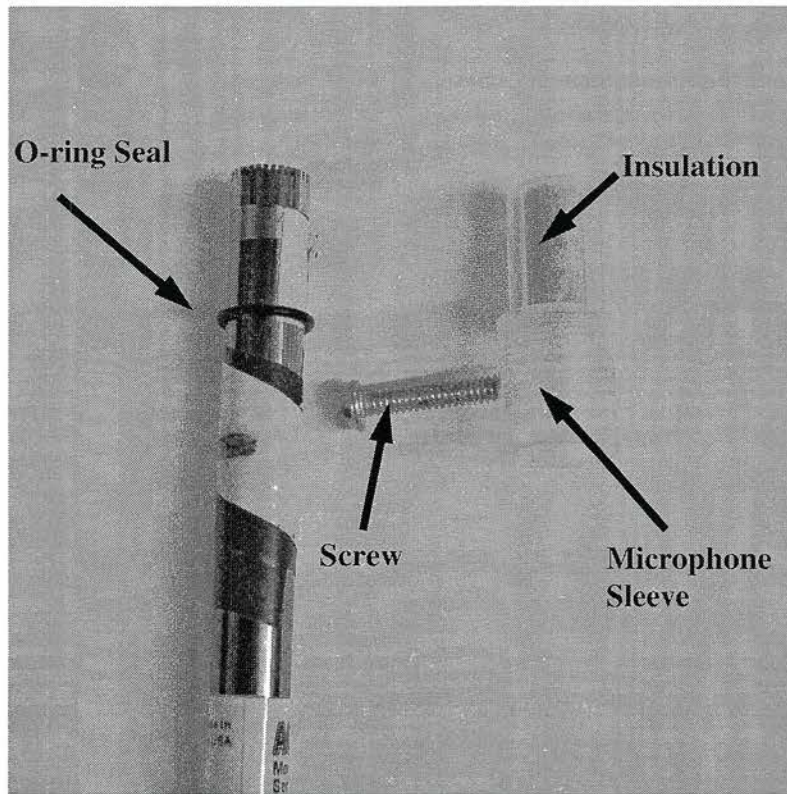


**Figure 2.14** Microphone, plastic sleeve assembly

The sleeve was designed with the assumption that the static pressure inside the duct was low, since the pressure drop across the fan was controlled by the fan room inlet. The sleeve may need to be redesigned if measurements are made with a static gage pressure inside the duct.

The values produced by the data acquisition system are pressure squared ( $\text{Pa}^2$ ). These values are converted to decibel scale,

$$L_p = 10 \text{Log} \left( \frac{P^2}{P_{ref}^2} \right)$$

where the reference pressure is  $2 \cdot 10^{-5}$  Pa, Bies and Hanson (2002). The one-third octave band data was then averaged over the nine room measurements, and separately the data over five of the duct measurements were also averaged. The pressure squared values are averaged,

$$Average = 10 \log_{10} \left( \frac{1}{N} \sum_{i=1}^N 10^{\frac{L_i}{10}} \right) \quad 2-7$$

where  $L_i$  is the  $N$  measured sound levels, Bies and Hanson (2002). In this case  $N=9$ .

## 2.2.2 Airflow Measurement and Estimation

An airflow station is placed downstream of the measurement room to record the airflow and the pressure drop. The airflow and the pressure drop are the two measured variables of the system. Both of these are controlled by the inlet restriction and the fan speed.

The airflow station contains six Dwyer pitot tubes. Each pitot tube is connected in sequence to a single Baratron, type 220BD-0010A2A-SP027 pressure transducer. The output voltage from the pressure transducer is input to a Keithley instruments Inc. 195A Digital Multimeter. Each pitot tube is 36" long and attached by a cross bar to keep them level. The six pitot tubes are connected by two bars that can be raised or lowered to specific points. The cross bars are suspended by two aluminum rulers that are mounted to the duct joint. These rulers are notched at locations to ensure that the pitot tubes are at the correct points for the pressure traverse shown in Figure 2.15. One bar clamps the pitot tubes at 18" below the tube inlet, so when the bar is positioned all the pitot tubes are positioned to the same point in the

duct. Each pitot tube is strapped to the second bar, this keeps the pitot tubes aligned at the same orientation, facing the flow. The airflow station is 6.4 duct diameters (16'-6") downstream from the transition exit and 1.9 (5') duct diameters upstream from the outlet plenum. The effective duct diameter of the downstream duct is 31 inches. The airflow station is connected to a rigid joint, assuming that this will minimize the effect of the air flow station on the duct wall vibration.

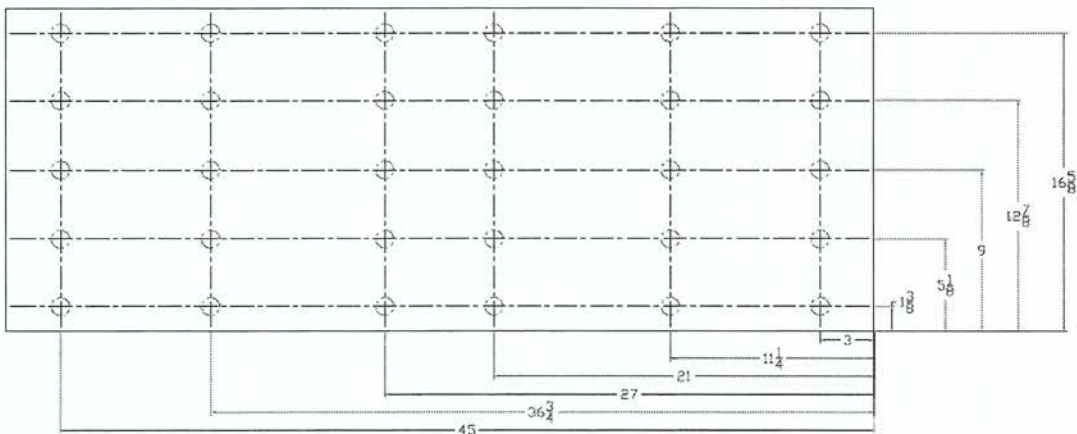


**Figure 2.15** Pressure Traverse locations

It is assumed in using these pitot tubes that the airflow is straight and gives a good value of the velocity pressure at that point. ASHRAE Fundamental (2005) gives a reliable pitot tube configuration that records a total of 30 local pressure drops throughout the duct. The locations of the 30 are shown in Figure 2.15. This gives the velocity pressure of the air at each point of the traverse. The voltage signal from the pressure is calibrated using,

$$p_w = 1.0838 * mV \quad 2-8$$

where mV is the voltage in milli-volts.

The pressure values are averaged, and the average is used to calculate a volume flow rate of the airflow through the duct in feet per minute,

$$Q = C(W \times H) \sqrt{p_w / \rho} \quad 2-9$$

Where:

Q = Airflow in (ft<sup>3</sup>/min)

p<sub>w</sub> = Velocity Pressure (lbf/in<sup>2</sup>)

C = Correction Factor 1096.5

ρ = Air Density (lbm/ft<sup>3</sup>)

H = Duct Height (ft)

W = Duct Width (ft)

The air density is assumed to be at atmospheric conditions 0.0739 lb<sub>m</sub>/ft<sup>3</sup>

### 2.2.3 Pressure Drop Measurement

The pressure drop across the fan is estimated not measured. The static pressure in the room can be measured with relative ease through a pressure tap in the fan room. However the outlet of the fan does not give a good indication of the pressure rise. ASHRAE standard 51 (1999) states that to measure the pressure rise across a fan the taps must be at least an 8.5 duct diameter distance away from the fan. That would require the fan to always be at least 17 feet away from the elbow. Obviously this is not possible with discharge configurations being tested. There are a number of tests where the fan is required to be directly against the elbow. Therefore the static pressure of the duct system is measured at the airflow station.

There are three pressures marked in Figure 2.16, P<sub>1</sub> is the fan room, P<sub>2</sub> is the fan outlet, and P<sub>3</sub> is at the airflow station. The measured pressure drop, Δp<sub>meas</sub>, is the difference between the fan room and airflow station pressures,

$$\Delta p_{meas} = P_1 - P_3 \quad 2-10$$

However, the desired value is the pressure drop across the fan,

$$\Delta p_{fan} = P_1 - P_2 \quad 2-11$$

Since  $P_2$  can not be measured the measured pressure drop is considered as the sum of the pressure drop across the fan, and the pressure drop across the duct between the air flow station and the fan outlet,

$$\Delta p_{meas} = \Delta p_{fan} - \Delta p_{duct} \quad 2-12$$

The measured value of  $P_3$  was taken by the pitot tubes at the airflow station. Each pitot tube has two measurements of pressure a velocity pressure and a static pressure. The static pressure is used for these measurements. The static pressure from six pitot-static tubes are taken and averaged to get  $P_3$ .

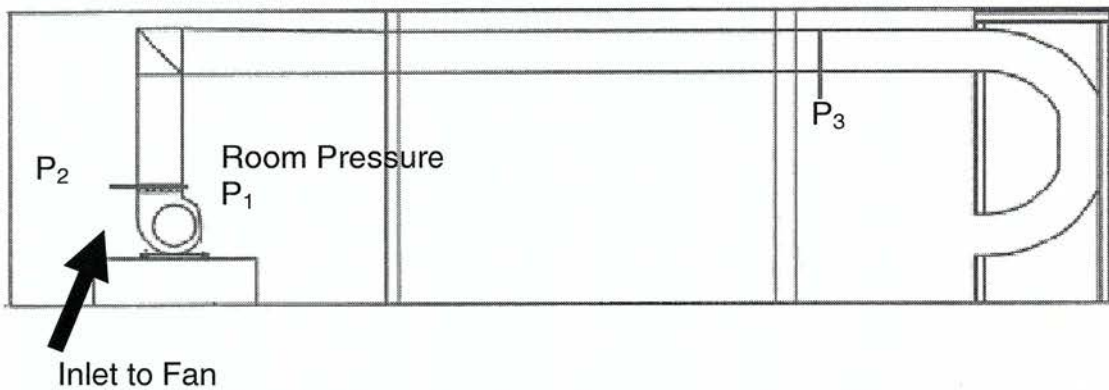


**Figure 2.16** Location of the pressure drop measurement.  $P_1$  and  $P_3$  can be measured, while  $P_2$  must be estimated.

In order to use equation 2-12 to solve for the  $\Delta p_{fan}$ , the value for  $\Delta p_{duct}$  must be estimated. The duct system includes the elbow, the transition, 16'-6" of duct length and any duct diameters between the fan and elbow (depending on the configuration). Using formulators by ASHRAE Fundamentals (2005), the value for  $\Delta p_{duct}$  can be estimated as,

$$\Delta p_{duct} = \left( \frac{12fL}{D_h} + \sum C \right) \rho \left( \frac{V}{1097} \right)^2 \quad 2-13$$

where:

$\sum C$  = the summation of the local loss coefficients (0.12 for the elbow, 0.32 for transition)

$f$  = friction factor

$L$  = Duct length

$D_h$  = Equivalent duct diameter

$V$  = Air Velocity

Equation 2-14 is based on local loss coefficients, friction factors for each section of the duct, and the air velocity. The local loss coefficients for the elbow and the transition were obtained from ASHRAE Fundamentals (2005). The elbow inlet and outlet dimensions are equal, and the turning vanes are spaced evenly apart and have a correction factor of 0.12. The transition piece has an inlet of 19.4" x 26" and an outlet of 18" x 48", with a 4:1 slope (14° angle). A correction factor for the transition piece is given in the ASHRAE Fundamentals (2005) as 0.32.

The friction factors for the large must also be estimated. There are two sections that must be analyzed each time the large duct and the small duct. The friction factor can be calculated using,

$$\frac{1}{f^{0.5}} = -2 \log \left[ \frac{12\epsilon}{3.7D_h} + \frac{2.51}{\text{Re} f^{0.5}} \right] \quad 2-14$$

which can be simplified to,

$$f' = 0.11 \left( \frac{12\epsilon}{D_h} + \frac{68}{\text{Re}} \right)^{0.25} \quad 2-15$$

$$\begin{array}{ll} \text{If } f' \geq 0.018: & f = f' \\ \text{If } f' < 0.018: & f = 0.85f' + 0.0028 \end{array}$$

where

$\epsilon$  = material absolute roughness factor, ft

Re = Reynolds number

f = friction factor

The average air velocity required for the above calculation is determined as follows

$$V = C\sqrt{p_w / \rho} \quad 2-16$$

Equations 2-13, 2-15, and 2-16 along with the tabulated values were used to estimate the pressure drop,  $\Delta p_{duct}$ , across the duct section. Equation 2-12 along with the measured pressure,  $\Delta p_{meas}$ , was used to estimate the pressure rise across the fan,  $\Delta p_{fan}$ .

#### 2.2.4 Fan and Motor Vibration Measurements

As stated previously, the fan and motor assembly are mounted on a rigid mounting base that is supported by a set of isolation springs to reduce the effect of vibration. Many imbalances can be caused in the system, and each aspect of the system was balanced individually. For example, between the fan and motor shaft, the coupler was designed to limit the imbalance that was caused by any misalignment between the motor and fan shafts. Despite these efforts, there are vibrations throughout the system. Therefore, the vibrations of the system needed to be measured because vibrations at the fan and motor assembly can cause noise in the downstream duct system. Mechanical vibrations can resonate through the ductwork, floor, walls or other structures. It must be certain that the noise that is measured in the measurement room is only coming from the aerodynamic effects at the outlet of the fan and not from the vibration effects that are caused by the fan or motor.

The required measurement is a peak velocity. Since it was unknown in what direction the highest vibration would occur, three axes were be measured with respect to the

fan orientation, shown in Figure 2.17. The X-Axis runs in plane with the duct work. The Y-Axis runs along the coupler shaft between the fan and motor. The Z-Axis runs perpendicular to the floor. The measurements were taken at two locations, one on the fan and the motor. Fan vibrations were measured on the ¼" steel plate that the shaft bearings are mounted to, and the motor vibrations were measured on the motor base.

The vibrations were measured with a tri-axial PCB Piezotronics shear accelerometer model # 356A15. The signal was sent through a PCB Piezotronics ICP Sensor Signal Conditioner, Model 485A22. This signal was in turn sent to the same Pulse data acquisition system as the sound levels, B&K Pulse Data Acquisition Unit Type: 3560C.

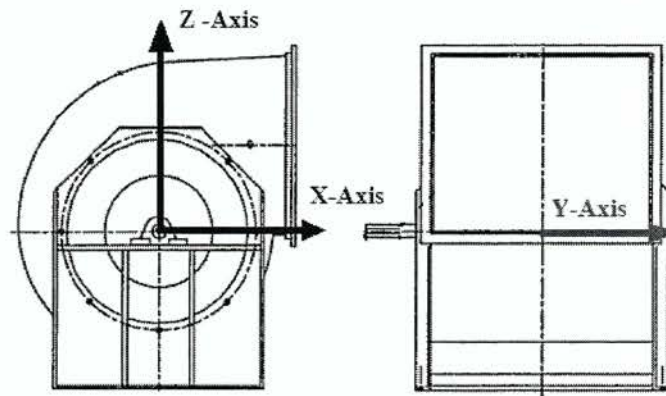


**Figure 2.17** Accelerometer Axes

The RFP calls for tri-axial peak velocities at the bearings of both the fan and the motor; however, there were no good locations to mount the accelerometer by the motor bearings. The base was used instead as shown in Figure 2.18.

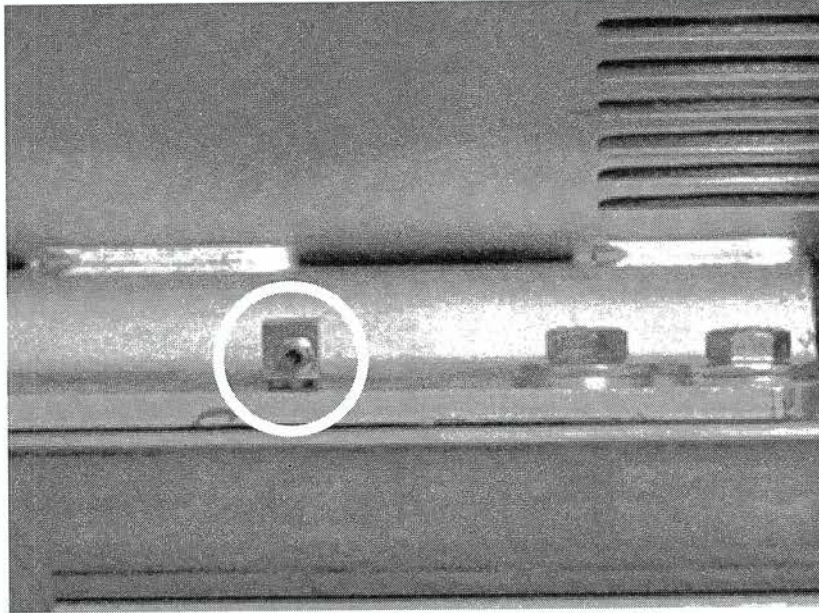


**Figure 2.18** Mounting Location of Tri Axial Accelerometer on the Motor

The accelerometer location on the fan was mounted on the shaft that supports the bearings as shown in Figure 2.19.

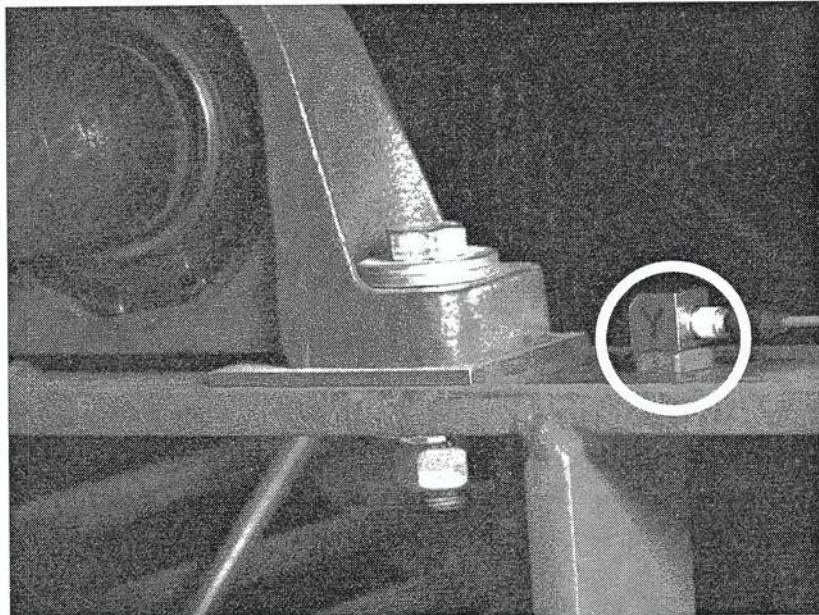


**Figure 2.19** Mounting location of Tri Axial Accelerometer on the Fan

The accelerometer signal was time integrated to produce a velocity time signal. The discrete frequency spectrum of each signal was calculated and stored along with the time signals. The data was taken with the same Pulse system as described in the sound measurements section. The time signal recorded 8 seconds of data and the discrete frequency spectrum took 100 averages. The initial tests of Configuration 1, zero duct diameters, were run with the system recording two seconds of time signal. An example of the data recorded is shown in Figure 2.20 for the case with the fan operating at 90% wide open flow and a pressure drop of 1.0 inches of water. The absolute values of the velocities are taken in order to obtain the magnitude. The peak velocities are the largest peaks observed in the time signals shown in Figure 2.20. For the data in Figure 2.20, the peak values that would be reported is 1.04 inches second, as seen in the y-axis fan time signal.

When looking at the narrow band frequency, the data acquisition system records the same frequencies as in the sound measurements. The recorded frequencies in the narrow band are 0 to 1,000 Hz for the configuration 1 and no duct diameters. There are 1600 lines for this case. For configuration 1, 1 duct diameter before the duct system the recorded frequencies were reduced to 0 to 800 Hz and 3200 lines. For the remainder of the configurations, the frequencies recorded are 0 to 800 Hz, and 6400 lines. The corresponding narrow band frequency spectrum of the configuration 1, zero duct diameters is shown in Figure 2.21.

It can be seen from the peaks in Figure 2.21 that the vibrations had very distinct peaks in the frequency while sound data had very broad band changes. These sets of data are recorded to compare with the sound data frequency spectra

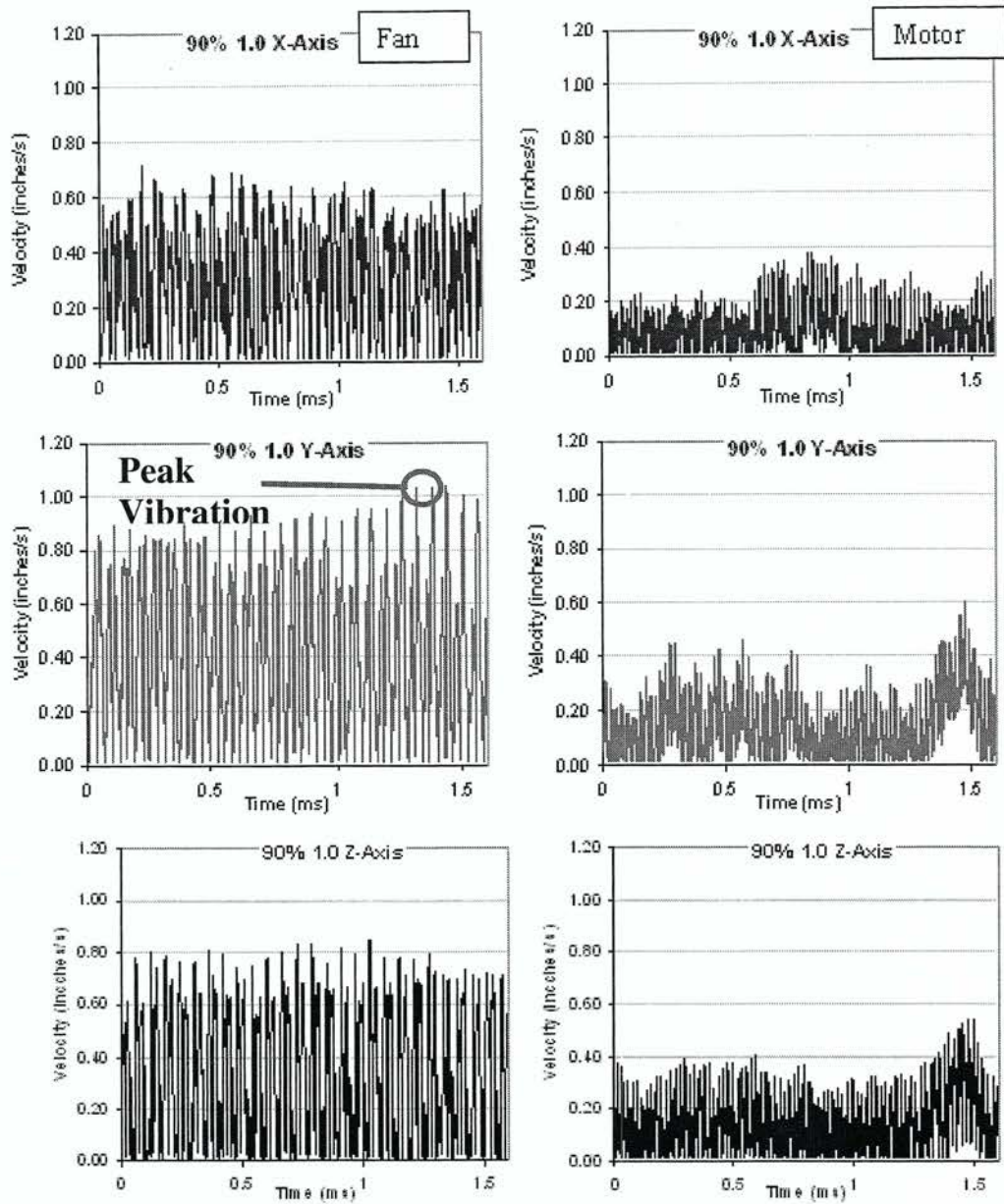


**Figure 2.20** Magnitude of the velocity time signals recorded by the data acquisition system.

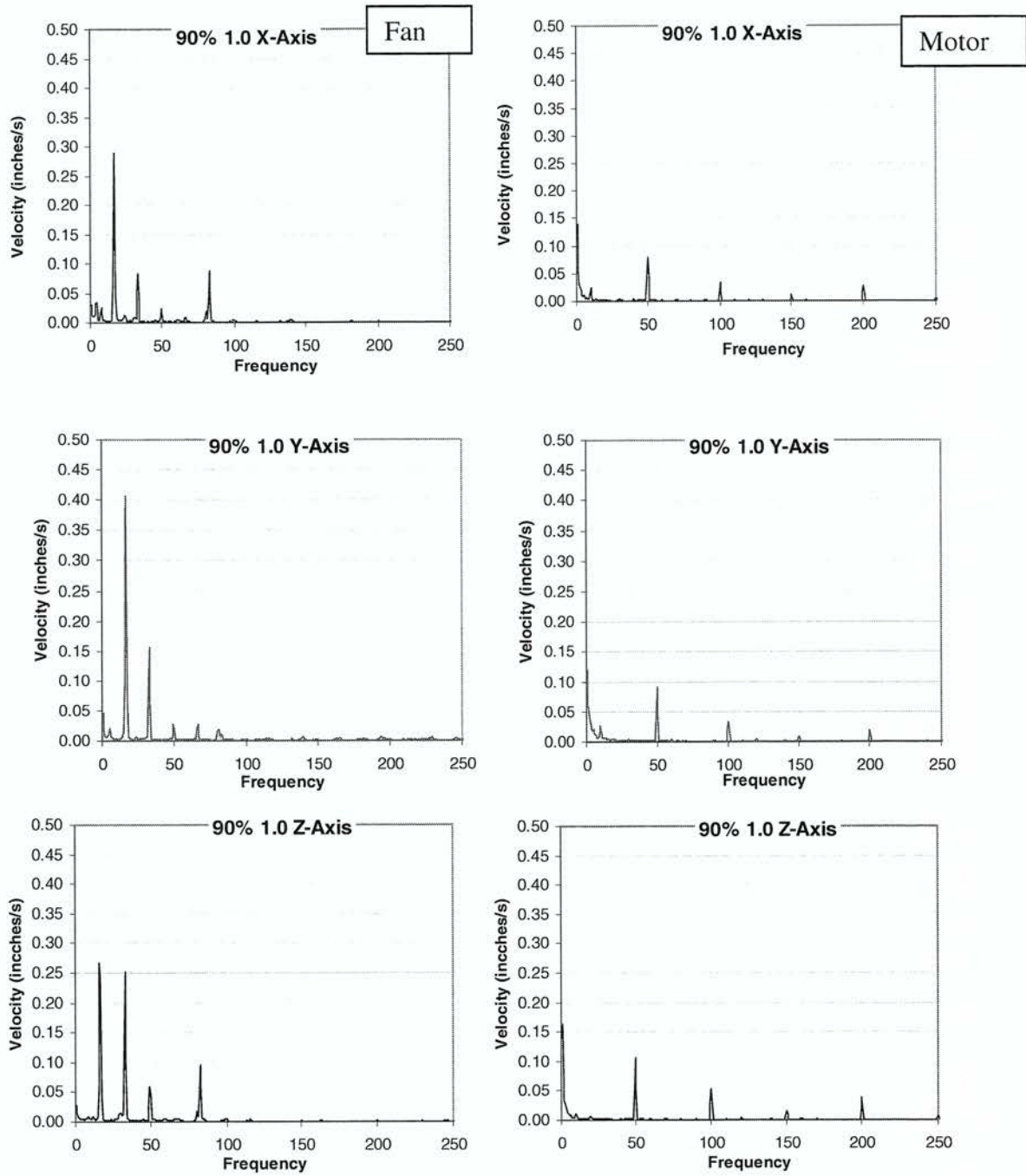


Figure 2.21 Velocity Frequency Spectra of the fan and motor.

### **2.2.5 Additional Measurements**

The variable speed drive (VFD) can be used to obtain some of the operating parameters of the system. The speed of the motor in RPM, the current drawn by the motor and the voltage motor were taken from the output display of the VFD. The fan speed was assumed to be the same as the motor. The current and voltage can be used to calculate the brake horse power of the fan. The motor runs at an efficiency of 93.6% with a performance rating of 80% when operating at 1180 RPM. The performance factor may change depending on the motor speed. The motor draw can be related to the brake horsepower of the fan; however, there is an additional correction factor that must be included in the calculation. These calculations were not performed for this thesis but could be implemented with all the available data.

### **2.3 Method of Test**

A method of test was developed to collect the data for the system because repeatability and consistency between tests is a large concern. It is critical that a concise methodology was followed in determining what operating parameters the fan would run at. A major concern for the ASHRAE committee is how the different operating conditions are going to be compared. With the system changing regularly, a method of test needed to be developed in order to determine the operating points and to ensure that they are the same for each configuration. The same applies for the sound pressure level tests. A methodology was developed for how the sound tests were taken to keep the measurements as uniform as possible without any external influences on the measurement.

The vibration measurements were performed at two locations and the system was run through the operating conditions in no particular order. The pressure drop measurements were taken at the airflow station in no particular order.

### 2.3.1 System operating points

A concern of the ASHRAE Committee was whether measurements at one condition could reasonably be compared to measurements at another condition. The calculated conditions in Table 2.2 are the conditions that the system is attempting to achieve. The pressure drop estimation is not fully trusted because the flow conditions are not ideal and because the pressure drop is estimated and not measured. The trusted values in this case are the measured values: the fan speed and the volume flow rate. Therefore, ensuring that the system was always operating at a given point required that the flow rate and fan speed measurements were constant.

To obtain the desired operating points, two different variables need to be set. They are the inlet restriction and the fan/motor speed. The first variable that was set was the inlet restriction, which sets the %WOF curve, Figure 2.22. To do this, the fan laws from Equations 2-4 and 2-5 were trusted, and the fan was set to the desired speed. The inlet restriction was then changed to achieve the desired air flow rate. The inlet restriction was now set for the rest of the operating points at those %WOF cause. The speeds that set the %WOF, along with the pressure drops that they represent were:

- 986 rpm for 90%, 1.0 inch of water
- 712 rpm for 80%, 1.0 inch of water
- 916 rpm for 60%, 2.5 inches of water
- 929 rpm for 35%, 2.5 inches of water

The rest of the operating conditions are set at the remaining pressure drops. This pressure drop again depends on the air flow rate. With the inlet restriction set, the RPM was changed until the desired airflow rate was achieved. This fan speed set the different pressure drops of the operating states. The first configuration with one duct diameter to the transition inlet was considered the baseline condition. The measured values for these were used as the base case and the rest were modified off of them, Table 2.3.

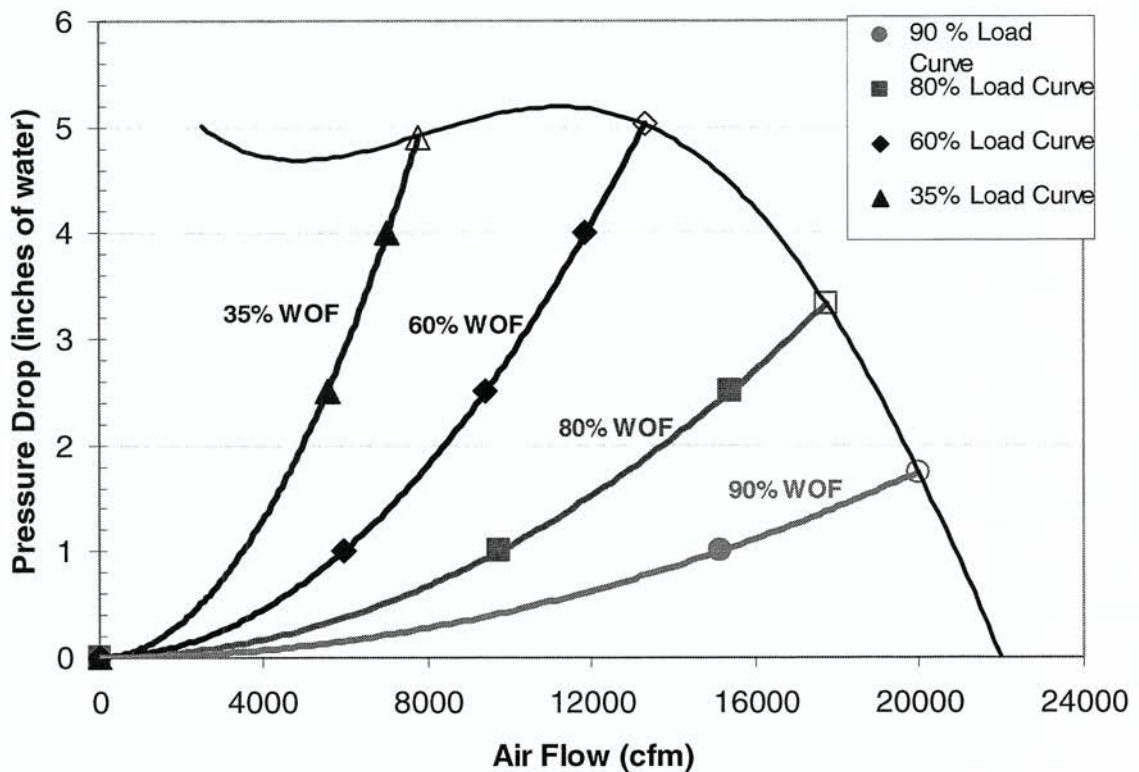


**Figure 2.22** Operating points set points along the fan curve.

When the configuration was changed the operating conditions needed to be reset. This process was similar to the one previously described. The fan speeds used from Table 2.2 are reused; the inlet restriction was changed to obtain the desired volume flow rate

**Table 2.3** Measured Operating Points of the Baseline Configuration

% of Wide Open Flow (%WOF)	Fan Pressure Drop (inches water), Fan Laws	Estimated Fan Pressure Drop (inches of water)	Fan Speed (rpm)	Volume Flow Rate (CFM)
90%	1.00	1.4	989	15,154
80%	1.00	1.0	713	9,742
	2.50	2.6	1,146	15,407
60%	1.00	0.8	554	6,014
	2.50	2.2	913	9,458
	4.00	3.5	1,150	11,865
35%	2.50	2.6	932	5,353
	4.00	4.2	1,194	6,671

Once the load curves were set, the airflow rates that was from the baseline configuration (no elbow, front blast, one duct diameter) were used to set the operating conditions of the rest of the configurations.

### Example of setting operating point

In Figure 2.23, four of the operating points were circled. These were the operating points that set the %WOF curves that the system follows. Each of the %WOF curves were a function of fan speed. Once one of the operating points was found on that load curve, changing the rpm will move along it. For this reason, setting the %WOF curve was done first. In Figure 2.24 the 60% WOF curve was set by running the fan at 913 rpm, and the inlet was then raised or lowered until the CFM comes within  $\pm 1\%$  of the load curve (for the 35% WOF curve the CFM was within  $\pm 2\%$ , because of the lack of control over the VFD). Then the rpm was increased or decreased until the CFM of the remaining operating points was within  $\pm 3\%$  of the desired value (again the 35% WOF curve was within  $\pm 6\%$  of the CFM because of the lack of control on the VFD).

### 2.3.2 Sound Pressure Level Tests

The sound pressure levels were taken with the data acquisition system. Two measurements can be taken at a time in an array of 16 microphone locations. This means that for each of the data sets 8 measurements must be taken. The process for taking the sound pressure levels are outlined here:

1. Keep the data acquisition system and computer system outside of the measurement room.
2. Calibrate the data acquisition system and microphones to the Pulse system.
3. Set microphone location for the desired test.
4. Cover the entrance of the measurement room with medium density fiberboard.
5. Take the current test.
6. Return to step 3 until all 8 measurements have been made.

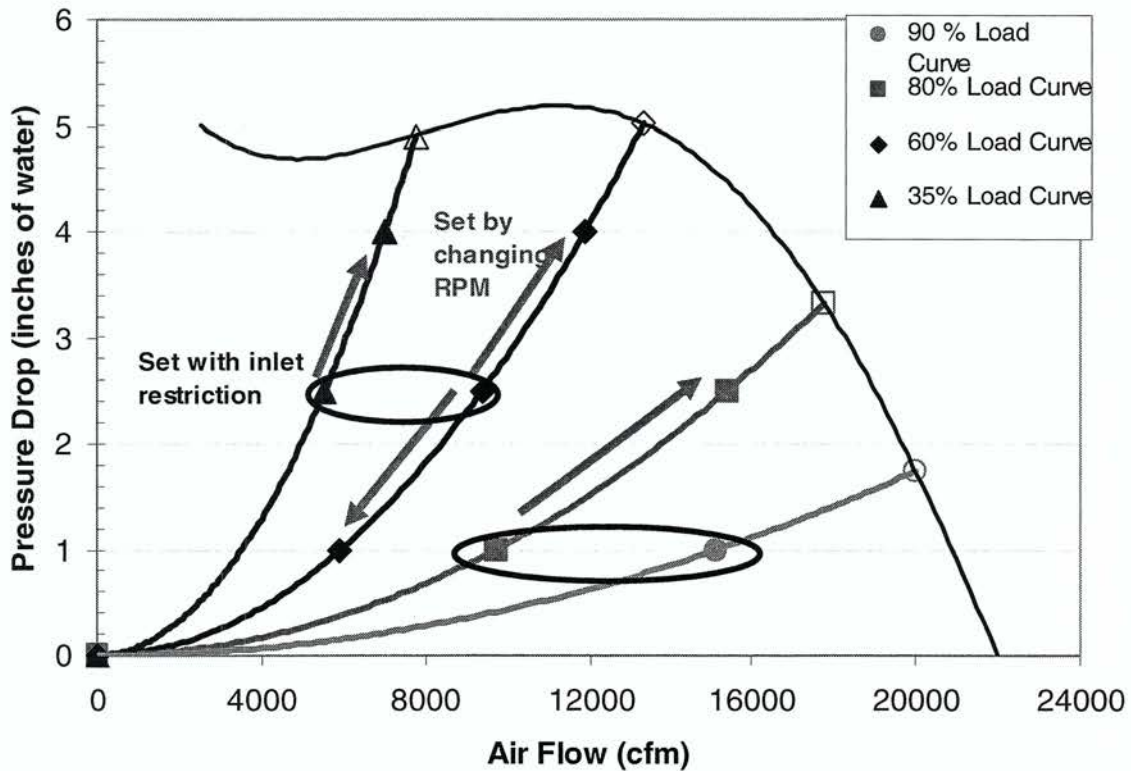


**Figure 2.23** Example of setting operating points. Operating points in the black circle are set with the inlet restriction. The remaining points are set by changing the fan speed that follows the red arrows.

The data acquisition system and the computer data acquisition computer was outside the room so that the fan of the computer does not interfere with the sound pressure levels. The computer fan may have a great effect on the background noise; and at low volume flow rates and low pressure drops the noise could skew the sound results. The data acquisition system was then calibrated at 1 kHz and 94.0 dB. This is a Bruel & Kjaer sound level calibrator Type 4230. This calibration was double checked on the data acquisition system to keep an accurate measurement.

The order in which the microphone locations that were shown in Figures 2.9 and 2.10 were measured is shown in Figure 2.24. The two channels were color coded for ease of use, channel 1 is RED, and channel 2 is YELLOW.

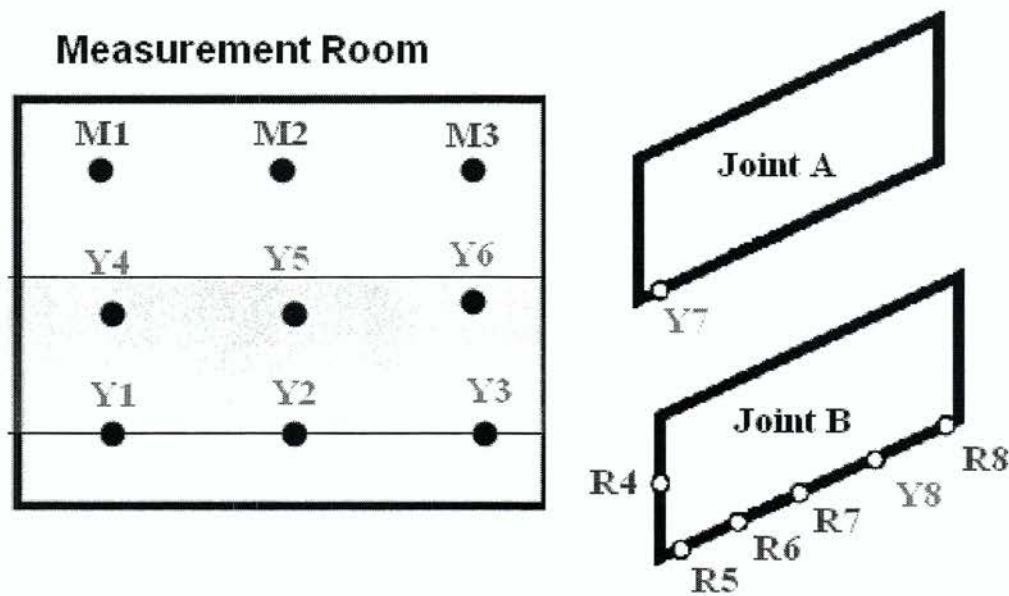


**Figure 2.24** The Order of the measurements, Channel 1 is in Red channel 2 is in Yellow.

As described in the acoustic isolation section, the entrance of the measurement room needed to be covered in order to ensure the proper transmission loss. This isolation was done with a 4' x 8' sheet of medium density fiberboard. Many of the tests were conducted with an

additional person in the measurement room who moves the microphones from location to location. Having a person inside eliminates having to move the fiberboard in between every measurement. The test taker on the inside needed to be conscious of sound tests and not make noise while testing was in progress. Once the test was finished the microphones can be moved to the needed locations.

## Chapter 3 Results: System Verification

After being constructed, the system's performance needed to be verified. First, it needed to be verified that the system could achieve the required conditions, and the resolution to which the flow conditions could each be set. The second task was to verify that the sound level could be accurately measured. Third, the measured fan shaft vibration were correlated to the results for potential contamination of the measured sound levels. The fourth task was to identify room and duct modes and compare them to potential contamination of the measured sound levels. Each of these four areas will be discussed separately.

### ***3.1 Operating Point Verification***

It needed to be proven that the operating point that was required in the ASHRAE RFP was attained in this system. The one of primary concern was the 90% WOF at 1.0 inches of water pressure drop. The reason that this was difficult to achieve was because if the measurement room inlet was too small, then there would not be free flow to the fan and motor assembly. This would make the 90% WOF load curve impossible to achieve.

The load curve was set by the volume damper at the inlet of the system. The maximum inlet area that the fan room can achieve was 19.36 square feet, with the volume damper removed entirely. The inlet must be cut off until the desired airflow is reached at the set RPM. A maximum airflow study was not needed for the test facility. The 90% WOF curve for the baseline configuration was set at an inlet area of 6.96 square feet. This allowed for enough room that the more turbulent configurations were able to expand in order to achieve their desired flow rates, the largest being configuration 4 ( $L/D=0,1,2$ ) at 9.9 square

feet and desired airflow rates of 15,200 CFM, 15,300CFM, and 15,200 CFM, respectively all at a fan speed of 988 RPM.

### 3.1.1 Air flow rate Repeatability

It was critical that the air flow rate be relied upon because the air flow rate was used to set the operating conditions. Two measurements were taken from the air flow station. One of these was taken at configuration 2, with 2 duct diameters to the elbow ( $L/D=2$ ). The fan and motor assembly was then torn down and rebuilt. The mounting base was taken off of the support base and the duct length was removed. The system was then rebuilt to configuration 2, with 2 duct diameters to the elbow ( $L/D=2$ ). The operating conditions were not reset according to the method of test in chapter 2.3. The fan was run at the same speed and at the same recorded inlet restrictions for each of the load curves. The results for the airflow repeatability are shown in Table 3.1. The maximum uncertainty is 1.3% difference between the initial measurement and the original measurement.

**Table 3.1** Flow rate repeatability.

	35%		60%			80%		90%
	2.5	4.0	1.0	2.5	4.0	1.0	2.5	1.0
Desired	5550	7020	5939	9391	11878	9732	15388	15147
First Trial	5840	7020	6100	9290	11800	9830	15300	15200
Second trial	5790	7060	6180	9360	11900	9750	15400	15400
Percent Difference	-0.9%	0.6%	1.3%	0.8%	0.8%	-0.8%	0.7%	1.3%

## 3.2 Sound Measurement Repeatability

The system verification involves the accuracy of the sound pressure level measurements and the influence that typical variation in the nominal value of the different

aspects of the system has on it. System repeatability was important to this study for analyzing the quality of the results. If the data was not repeatable, then the sound data becomes unreliable and one configuration cannot be compared with another. The ASHRAE RFP calls for an uncertainty of  $\pm 5$  dB from 16 through 50 Hz, and  $\pm 3$  dB above 50 Hz for the “baseline” measurements. In addition, the comparative measurements should not exceed  $\pm 3$  dB for all frequencies. The repeatability of the sound measurement system was found to be within  $\pm 1$  dB within a configuration.

There are two ways to define the uncertainty of a measurement system. The first is the precision of the measurement to a “true” value of what is being measured. The second is the repeatability of the measurement, and whether one measurement can be repeated to obtain the same result. The precision is important when dealing with the airflow and the fan speed. However, when dealing with sound, the precision was unimportant the change in sound level is what needed to be quantified. The exact level of the baseline was not as important as long as the difference between two measurements can be trusted. Therefore for sound, the difference was what was critical. As long as the measurements can be reliably repeated the difference can still be trusted. For this reason, the term uncertainty was assumed to pertain to the repeatability of the sound pressure measurement.

A repeatability analysis was done on the point measurement. The total sound pressure levels will average the sound over nine points in the room; the repeatability of each point will indicate the parameters most affecting the repeatability of the sound measurement.

The analysis of the repeatability was broken down to determine what causes the most amount of repeatability. The data acquisition system was calibrated before any tests are taken, however, there could be discrepancies in the signal or time variations at the

microphone location. For this reason, the repeatability of the measurements in the data acquisition system had to be found. The microphones were moved from one location to another eight times for a single operating condition. Even though every caution was taken to ensure that the microphone was always returned to the same spot, the microphone location and orientation could change the repeatability.

The fan speed was rarely changed in the middle of a sound test, however, the repeatability of changing the fan speed to one state and then back to another was analyzed. This repeatability was the measure of the systems ability to recreate the same steady state condition after a shift in the system rpm. The volume damper was measured to determine the repeatability in the positioning of the inlet then having the system repeatedly adjust to the inlet restriction in the same way. Finally all of the variables are changed and then returned to check the location by location repeatability. These variables were the data acquisition system, the microphone location, the motor and fan speed and the inlet restriction.

### **3.2.1 Repeatability of sound level measurement at a point**

There were a number of elements that could affect the repeatability of a single measurement. The first level of repeatability was the measurement system itself. This was simply the uncertainties within the measurement system. Multiple measurements were taken at three of the room locations. Each was left in the same location for three measurements. Table 3-2 shows the measurement location that had the highest level of repeatability. Each one third octave band was measured twice; these were the first three columns. The fourth column was the average of the two trials, and the fifth and sixth columns were the differences between the trials and the average.

The largest value was taken to have the most conservative estimation of the repeatability. As can be seen from Table 3.2 the largest value was 0.8 dB at the 16 Hz one third octave band and at the 40 Hz one third octave band. The other one third octave bands do not go above 0.3 dB difference from the average. Based on the data in Table 3-1 the maximum repeatability from measurement to measurement was  $\pm 0.8$  dB within the acquisition system.

**Table 3.2** The measurement repeatability from 16 through 250 one third octave bands

One-Third Octave Bands	Trial 1, Sound Pressure Levels (dB)	Trial 2, Sound Pressure Levels (dB)	Log Average of Trials 1 and 2, (dB)	Trial 1 – Average (dB)	Trial 2 – Average (dB)
16	66.3	64.8	65.6	0.7	-0.8
20	59.5	59.7	59.6	-0.1	0.1
25	54.2	53.6	53.9	0.3	-0.3
31.5	52.6	52.8	52.7	-0.1	0.1
40	62.5	64.0	63.3	-0.8	0.7
50	60.9	61.5	61.2	-0.3	0.3
63	64.1	64.2	64.1	-0.1	0.1
80	55.3	55.5	55.4	-0.1	0.1
100	53.0	52.6	52.8	0.2	-0.2
125	61.2	61.2	61.2	0.0	0.0
160	58.4	58.5	58.4	0.0	0.0
200	55.0	55.0	55.0	0.0	0.0
250	49.4	49.5	49.5	0.0	0.0

To check if this repeatability could be reduced, the time averaging was increased to one minute and then to two minutes. The same method was used to check these time averages at the three locations and then averaged. The repeatability was reduced to  $\pm 0.6$  dB, which was not considered a significant change.

Moving a microphone from one location and then moving it back to the same was checked to see if this had any adverse effects on the repeatability. This had no effect on the repeatability. The microphone locations are marked and should not cause repeatability in the

location, but in order to move the microphone, the door must be opened and the MDF sheet that covers it must be removed and replaced.

The next cause of repeatability that was checked was changing the motor speed and then returning it to the original speed. This did affect the repeatability. The airflow of the system obviously needs time to adjust. The repeatability in this case was increased to  $\pm 1.3$  dB for each measurement. The repeatability in the inlet restriction was checked to be certain the system adjusted to the restriction the same way each time. To do this, the fan speed had to be changed in order to reset the inlet restriction. Again, this seemed to have no impact on the repeatability of the system. Changing all of these and returning at a different time to check the total tolerance of each individual measurement the repeatability was  $\pm 2$  dB.

### **3.2.2 Repeatability of the Room Sound Level**

The repeatability of each point was known but the desired value was the repeatability of the overall room measurement. The reason multiple points are taken is to eliminate the repeatability of single locations. More locations gave a better average of the overall sound level; therefore, nine measurements are done in the room and then averaged.

The total repeatability of the system sound measurements was done by taking three sound measurements. Each test used a different testing organization. The first test was conducted with a constant operating point and rotating the microphones among the locations in the room. The second test was done with constant microphone locations and rotating among the operating points. The last test was done randomly with no order set methodology. This was done to make sure that the test organization had no effect on the repeatability.

Once these three test were taken, the results were averaged and the variance in dB was plotted.

Figure 3.1 shows the repeatability of three trials at the operating point 35% of the wide open flow, 2.5 inch pressure drop for the one third octave bands between 16 and 250 Hz. This example was chosen because it was consistent with all the operating points collected. From the data in Figure 3.1, an average repeatability of  $\pm 0.9$  dB is assigned. The 0.9 dB was obtained by the taking the highest peak that across the one-third octave bands. In the case of Figure 3.1, the highest peak (or largest distance away from the average) was at 20 Hz One third octave band. This gives the most conservative approximation for the repeatability.

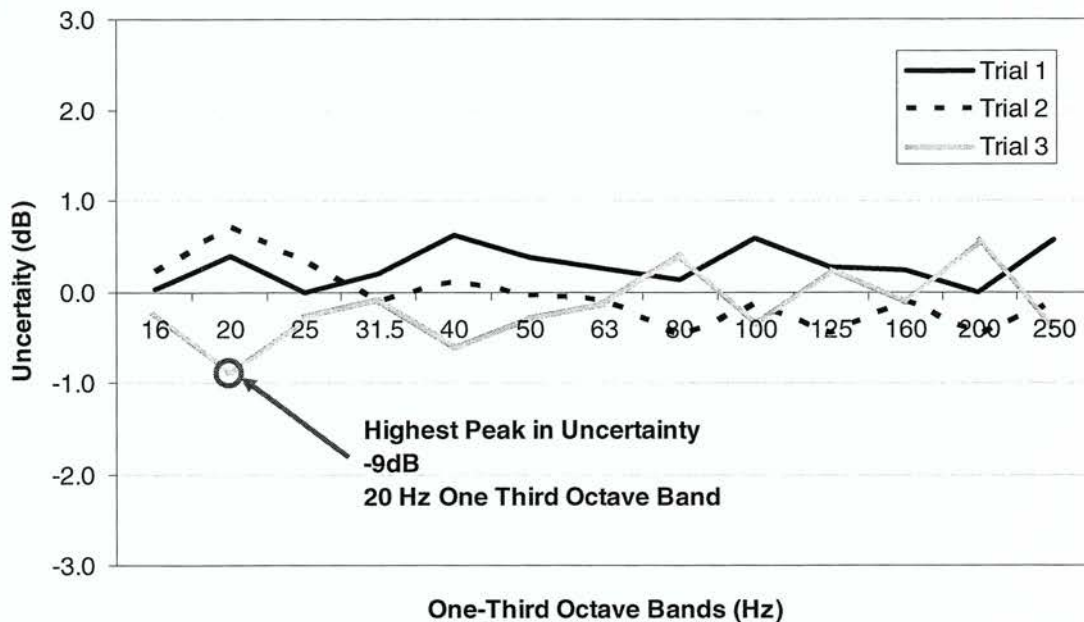


**Figure 3.1** Repeatability of the 35% WOF at 2.5 inch pressure drop

The one third octave sound level repeatability of all of the operating points was shown in Figure 3.2. It can be seen from these graphs that the only a few of the operating

points have high levels of repeatability. Of the operating points that do have a high level of repeatability, these did not occur at the entire range of one third octave bands.

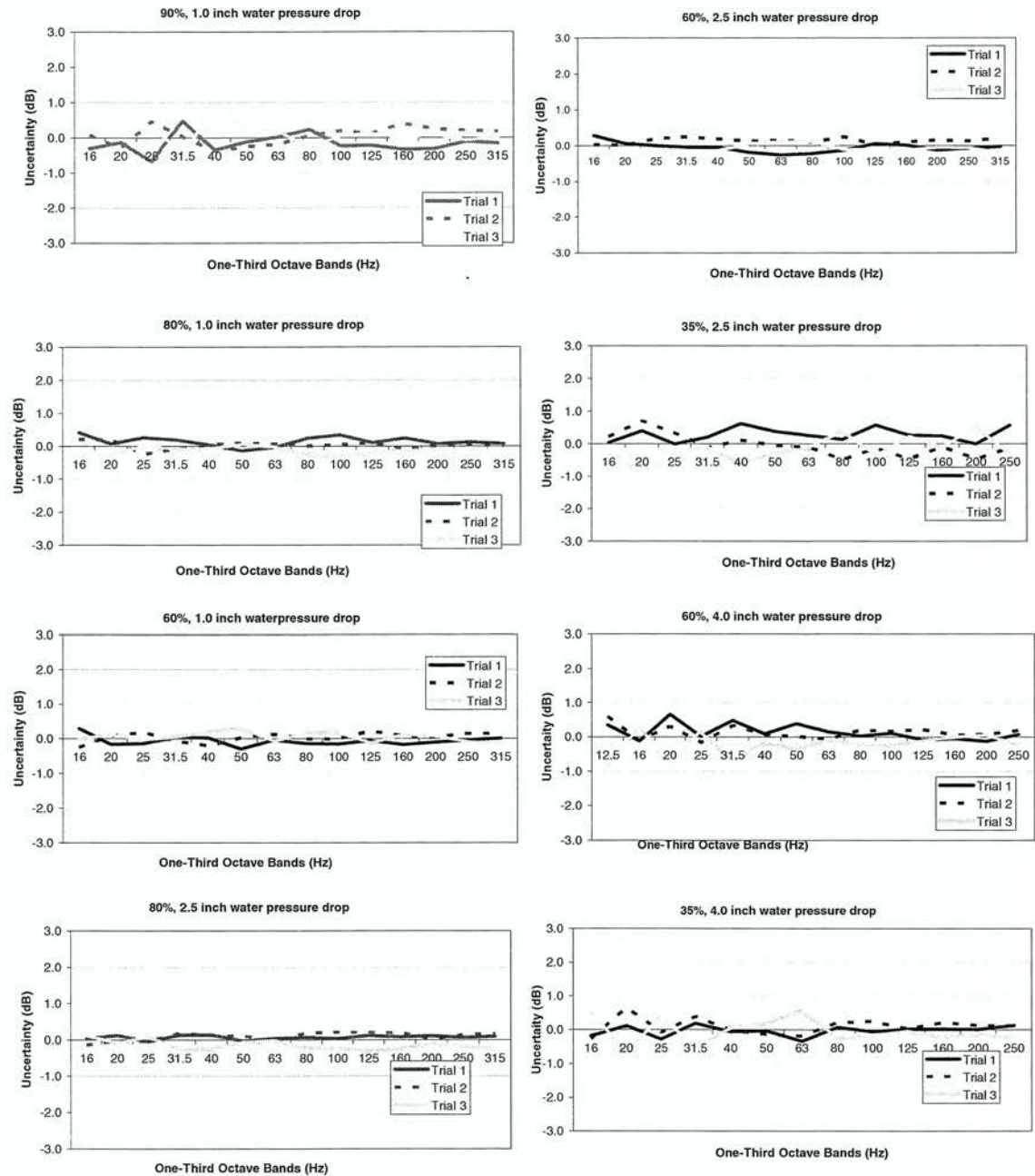


**Figure 3.2** Repeatability of the eight operating conditions of the fan at configuration 2, ( $L/D=2$ )

From these the maximum values were obtained and are shown in Table 3.3. These values were only for configuration 2 and with the fan two duct diameters ( $L/D = 2$ ) away from the elbow. The repeatability pertains to one measurement without changing the configuration or duct diameter. This was obviously within the level required by ASHRAE of  $\pm 3$  dB. This level of repeatability makes the comparison of sound levels more reliable, the noticed changes in the sound levels at the one third octave bands are up to 15dB.

**Table 3.3** Repeatability of Sound Measurements (dB)

90%, 1.0	80%, 1.0	60%, 1.0	80%, 2.5	60%, 2.5	35%, 2.5	60%, 4.0	35%, 4.0
$\pm 0.8$ dB	$\pm 0.6$ dB	$\pm 0.3$ dB	$\pm 0.3$ dB	$\pm 0.3$ dB	$\pm 0.9$ dB	$\pm 0.8$ dB	$\pm 0.7$ dB

### **3.3 Vibration and Balancing**

The vibration and balancing of the fan and motor was important to the system verification because the vibration in the duct can cause noise in the measurement room. The objective was to measure the aerodynamic effects on the noise level not the vibration effects. This section will cover the vibration peaks and the analysis of whether they are corrupting the sound data.

#### **3.3.1 Peak Velocities**

The vibrations were recorded in two ways, the time velocity and the frequency spectrum. In some of the cases, the data acquisition system was unable to obtain the frequency spectrum because of overload problems; however, time vibrations were obtained. For configuration 1 and the fan discharging directly into the system, the peak velocities in inches per second are shown in Figure 3.3. The highest peak velocity was 1.04 inches per second. Again, these were taken on both the fan and the motor. The peak velocities were

obtained from the time signal, and the highest absolute value of the time vibrations were recorded. These peaks were then plotted for each of the operating points and for both the fan and the motor. The RFP from AHSRAE required a maximum peak velocity in any direction to be 0.15 inches per second. Clearly this value was being exceeded by the system. Each of the system components were dynamically balanced from the respective manufacturers.

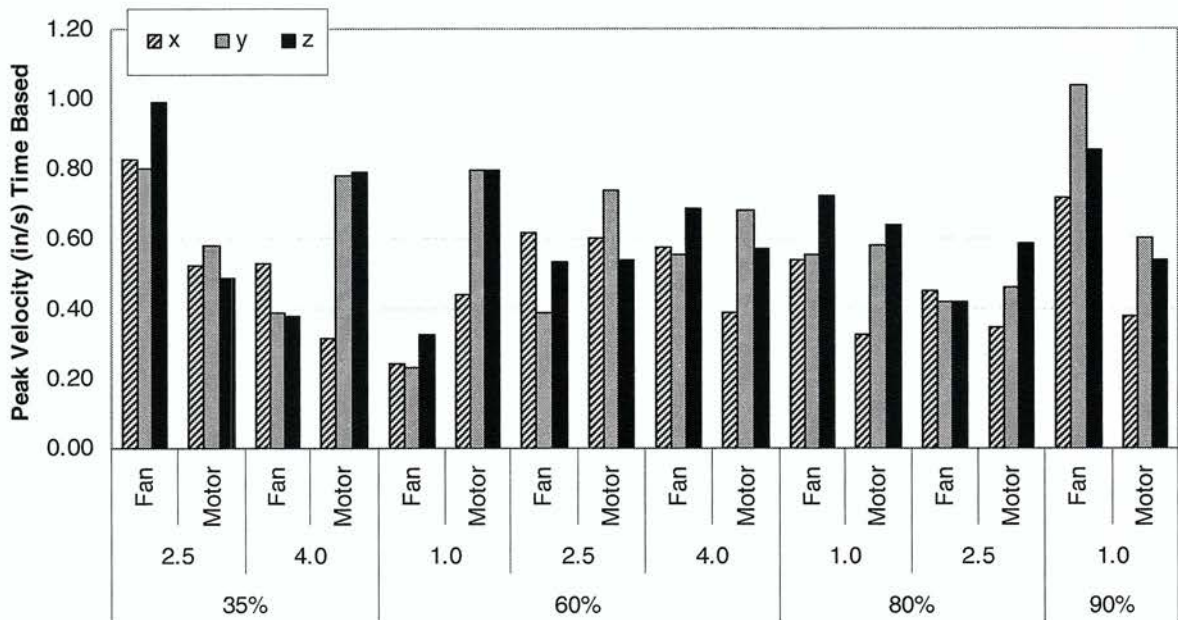


**Figure 3.3** Velocity peaks of the operating points for configuration 1, 0 duct diameters. The fan (solid) velocities show values that were taken by the fan shaft bearings. The motor (lined) velocities were taken on the motor.

An attempt was made to stiffen the support structure, and reduce the amount of vibration. Additional cross supports were added to the steel frame, along with mounting plywood to the fan side of the structure. The results of the reinforcing the structure is shown in Figure 3.4. The reinforcements had little effect on the system. In some conditions the system was improved, however in others conditions the velocities increased. These results

indicate that the vibrations cannot be reduced without significant changes to the support structure.

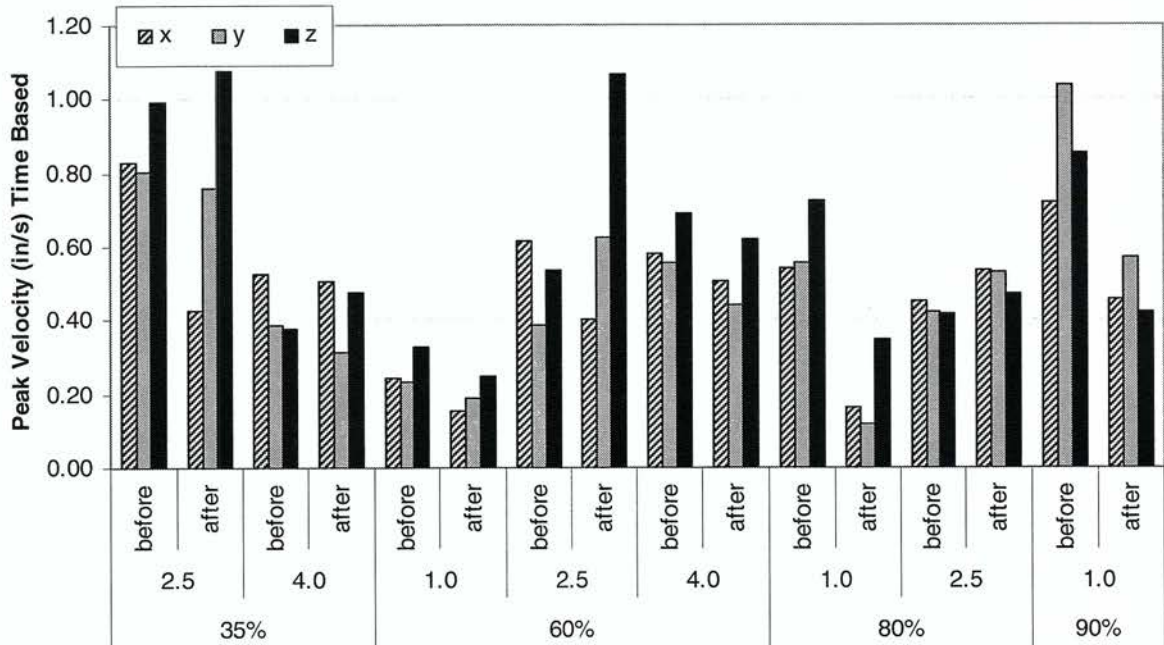


**Figure 3.4** Peak Velocities of each operating point. The before (solid) velocities were taken before the reinforcements were put in. The after (dashed) velocities were taken after the reinforcements were put in.

Figure 3.5 shows the measured peak velocities on the platform and the support structure. The motor and fan were mounted on the platform that was supported at the required heights by the support structure. The results show that the platform has lower vibration levels than the support structure, suggesting that the isolation springs help isolate the platform from the support structure. The results also implied that stiffening or increasing the mass of the support structure will not gain the required reduction to get the vibration below the required level.

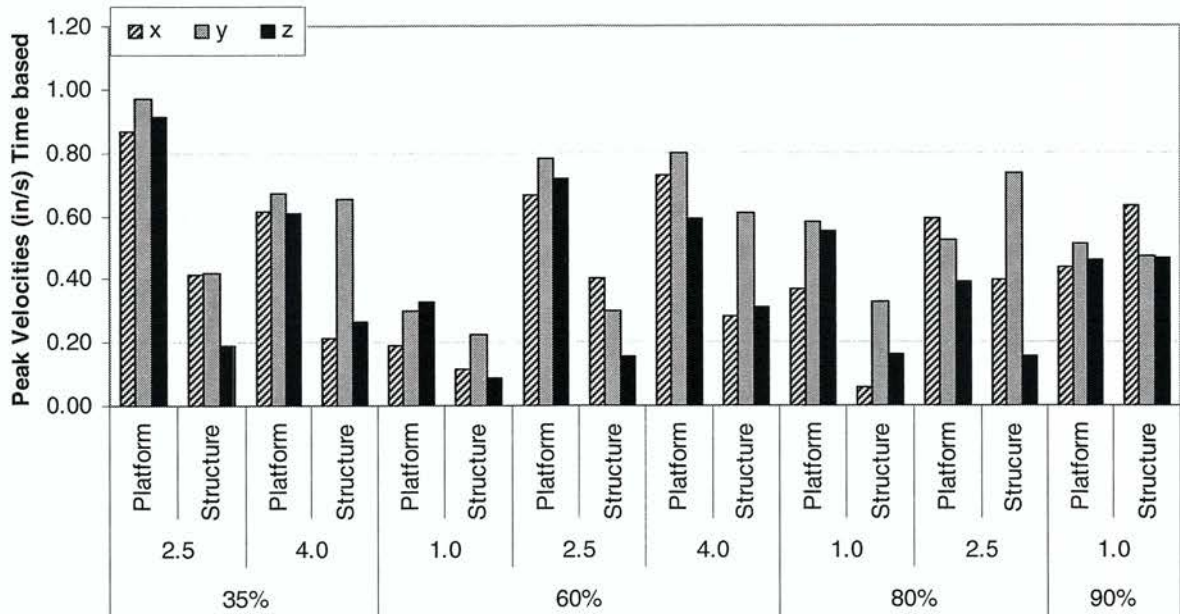


**Figure 3.5** Peak Velocities at the operating conditions. The platform (solid) is the peak velocities of the isolated mount structure that the fan and motor are directly mounted to. The structure (hatched) velocities are the frame that supports the fan, motor and platform.

### 3.3.2 Vibration Effect on Sound

A good way to verify where the vibrations were affecting the system was to look at the frequency spectrum of both the vibration and the sound levels. There were some specific frequencies that should be looked for when analyzing the vibration. The fan has 36 blades, therefore the blade passage frequency ranged from 345 Hz to 705 Hz for the cases concerned which was far above the peaks that were causing concern. Thus, the source of the peaks in the vibration response was not directly related to an interaction of each blade to an aerodynamic loading such as passing the cutoff in the fan shroud.

To find what frequencies are causing disturbances in the sound levels, the narrow band sound level frequency was looked at compared to the peaks in the vibration frequency. The vibrations generally correspond to the fan speed frequencies. The sound level frequencies had the highest peaks at the 4<sup>th</sup> and 8<sup>th</sup> fan rpm harmonics. These peaks reach up

to 13 dB greater than the rest of the frequency spectra. In Figure 3.6, the narrowband frequency spectra of 90% at 1.0 inch pressure drop are shown. In this figure, the major peaks occur at the 1<sup>st</sup>, 4<sup>th</sup>, 8<sup>th</sup>, and 9<sup>th</sup> harmonics. These were only slightly greater than the rest of the frequency peaks. Figure 3.6 was compared to the vibration frequency spectra in order to see if the frequency of the vibration peaks matched the frequency of the sound peaks. As can be seen from Figure 3.7, the vibrations and the sound do not correspond.

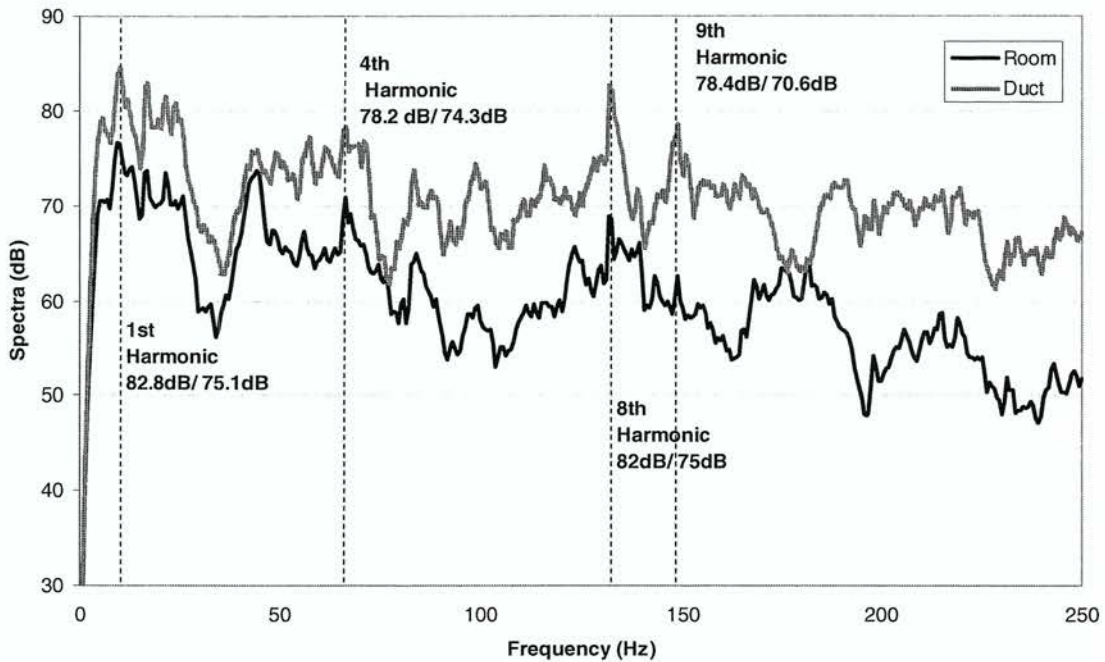


**Figure 3.6** 90% WOF 1 inch pressure drop, average discrete frequency spectra with fan RPM harmonics shown (fan frequency 16.5 Hz)

Table 3.4 displays each of the operating points that are tested, with the fan speed each of the operating point runs along with the fundamental frequency and the first two harmonics of that fan speed. The last section of the table lists the peak frequencies observed in the fan and in the motor.

The data in Table 3.4 shows that the fan vibration is dominated by the shaft rpm and harmonics while the motor vibration is typically at multiples of three times the shaft rpm. These results indicate that the motor and fan are effectively decoupled with the shaft coupler being used. In the case of the fan, the results in Table 3.2 also show that the vibration was dominated by a once per revolution imbalance in the fan and fan shaft assembly.

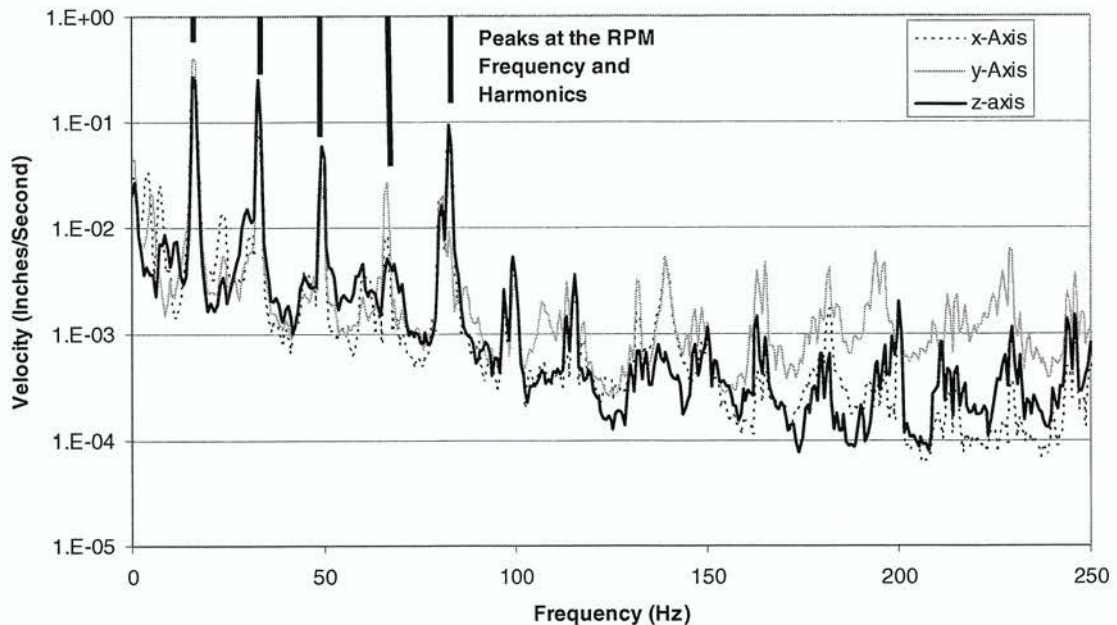


**Figure 3.7** Spectrum Vibrations of the Fan. The X-axis is the horizontal; the Y-Axis is the axial, the Z-axis is the vertical. 90% load curve at 1.0 inch pressure drop operating point.

The data in Table 3.4 shows that the fan vibration is dominated by the shaft rpm and harmonics while the motor vibration is typically at multiples of three times the shaft rpm. These results indicate that the motor and fan are effectively decoupled with the shaft coupler being used. In the case of the fan, the results in Table 3.2 also show that the vibration was dominated by a once per revolution imbalance in the fan and fan shaft assembly.

All of the operating points have been analyzed in the same way. The largest peaks consistently occur at the 4<sup>th</sup> and the 8<sup>th</sup> harmonic from the noise data. However, as seen in these examples, the peak vibration responses were not at the 4<sup>th</sup> and 8<sup>th</sup> harmonic. At the peaks in the vibration spectra, there was little or no effect on the sound data. According to a phone conversation with one of the ASHRAE committee members (Osborne 2005) vibrations are likely to affect the 2<sup>nd</sup> harmonic. There was no effect at the second harmonic in all but two of the operating conditions.

**Table 3.4** Operating Points, fan speed in terms of rpm and frequency and Peak frequencies

Operating Points		Fan Speed		Peaks in Frequency Spectra	
% WOF	$\Delta P$ (inch)	RPM	Hz (fundamental + two harmonics)	FAN	MOTOR
35%	2.5	932	15.5, 31.0, 46.5	15.6, 30.6, 45	16.9, 33.1, 46.9
	4.0	1,174	19.6, 39.2, 58.8	19.4, 30.6, 39.4	58.8, 118.2, 176.9
60%	1.0	594	9.9, 18.8, 29.7	10.0, 20.0, 30.0	30.0, 60.0, 120.0
	2.5	913	15.2, 30.4, 45.6	15, 30.6, 45.6	15.6, 30.6, 46.2
	4.0	1,170	19.5, 39.0, 58.5	19.4, 30.6, 38.8	58.8, 118.1, 176.9
80%	1.0	713	11.9, 23.8, 35.7	11.9, 23.8, 30.6	36.2, 71.9, 143.8
	2.5	1,126	18.8, 37.6, 56.4	18.8, 37.5, 51.9	56.9, 113.8, 171.3
90%	1.0	988	16.5, 33.0, 49.5	16.3, 33.1, 49.4	50.0, 100.0, 150.0

It should be noted that the fan blades were supported by four rods, which interfere with roughly one third of the blade length, and these fan rods extend over  $\frac{3}{4}$  of the inlet causing a large inlet disturbance 4 times each rotation as shown in Figure 3.8. This was strong evidence that the 4<sup>th</sup> and 8<sup>th</sup> harmonics that are seen in the noise spectra were results of aerodynamic disturbance of the fan instead of a vibration problem.

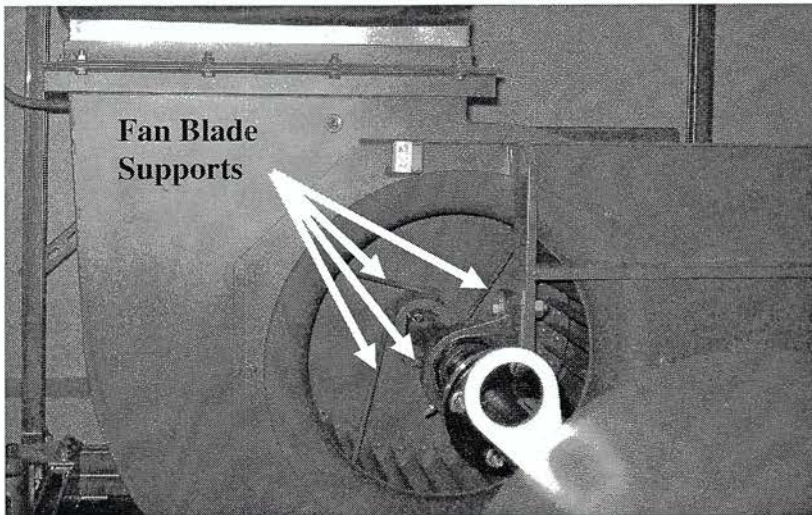


**Figure 3.8** Fan Cage Supports

### **3.4 System Modes**

The modes in the system needed to be identified and eliminated if possible or isolated in the recorded data. If these modes exist within the measurement room, the one-third octave band that includes the frequency will not be accurate. The measurement room dimensions were relatively small. The reason for this is because room modes are based on room geometry and with a small room there are likely to be fewer room modes.

The modes that have been identified can be seen in the measured sound spectra. Further, the variation in the sound levels at the frequencies of the identified modes also had a spatial pattern typical of the modes in the duct and room. However, none of the modes identified have a great impact on the sound results.

#### **3.4.1 Room Modes**

To determine the presence of room modes in the data, predictions were made of the frequency of the modes below 250 Hz. The modes are approximated assuming a rigid wall

rectangular room model Bais & Hansen (2002). The X, Y, and Z were the axis of the room and directions of the modes,

$$f_n = \frac{c}{2} \sqrt{\left(\frac{n_x}{L_x}\right)^2 + \left(\frac{n_y}{L_y}\right)^2 + \left(\frac{n_z}{L_z}\right)^2} \quad 3-1$$

The estimations were taken from equation 15, where  $L_x$ ,  $L_y$  and  $L_z$  are the dimensions of the room. The X axis follows the duct along the room, the Y axis was perpendicular to the duct, and the Z axis was along the vertical of the room. A speed of sound of 343 m/s was used. Table 3.5 shows the frequency and x, y, z mode number for each mode.

**Table 3.5** Predicted Modes in the Measurement Room

X	Y	Z	Freq	X	Y	Z	Freq
0	1	0	42	2	2	1	150
0	0	1	54	2	3	0	168
1	0	0	56	3	0	0	169
0	1	1	68	3	1	0	174
1	1	0	70	2	3	1	177
1	0	1	78	3	0	1	177
0	2	0	83	3	1	1	182
1	1	1	88	3	2	0	188
0	2	1	99	3	2	1	196
1	2	0	101	3	3	0	210
2	0	0	113	3	3	1	217
1	2	1	114	4	0	0	225
2	1	0	120	4	1	0	229
2	0	1	125	4	0	1	231
0	3	0	125	4	1	1	235
2	1	1	131	4	2	0	240
0	3	1	136	4	2	1	246
1	3	0	137	4	2	1	246
2	2	0	140	4	2	1	246
1	3	1	147	4	2	1	246

The narrow band spectra in the room were then analyzed to see if any of the peaks in the spectra could be associated with the predicted room modes. Figure 3.9 shows the discrete frequency spectra for configuration 1. There were peaks in the spectra, and the ones marked in Figure 3.9 were close to the frequencies of modes identified in the model.

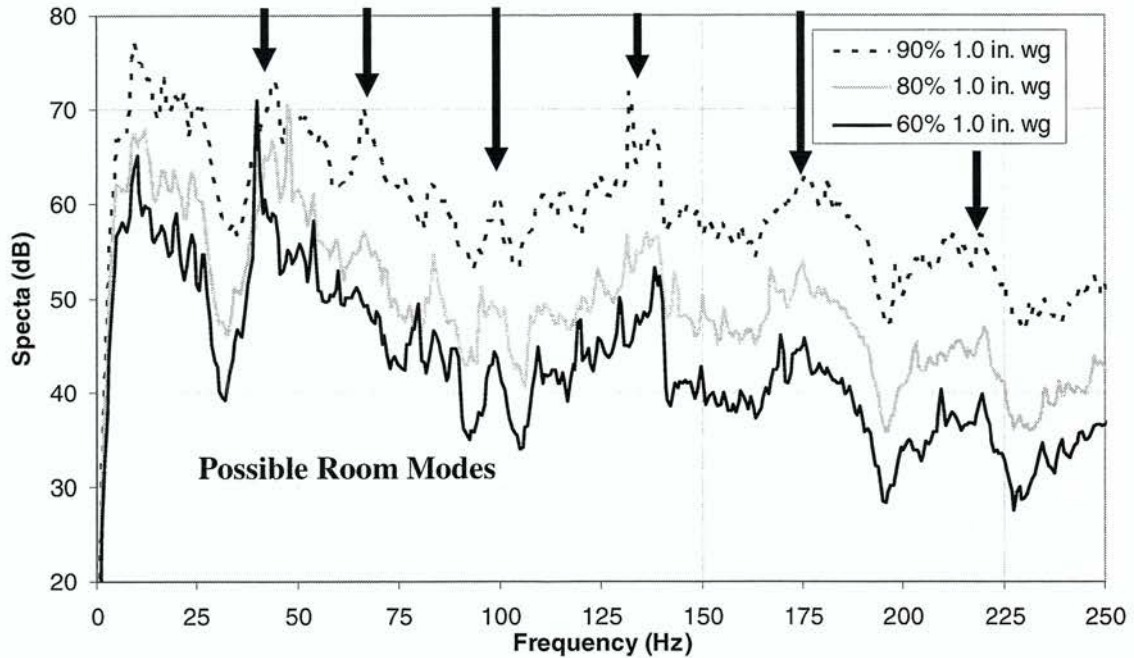


**Figure 3.9** Average Discrete Frequency Spectra in the Measurement Room, Configuration 1, no distance between fan and elbow,  $\Delta P= 1.0$  inch

Each of these frequency ranges were checked to see if any of them appeared as a room mode. The modes can be seen in greater detail by analyzing the distribution of the sound levels throughout the room. The grid of nine measurement locations can be plotted as a sound level distributing chart. Figure 3.10 is a sound level distribution chart of the measurement room at 68 Hz. In this figure, the nine measurement location are marked as the exterior of the room. The room itself extends past these marks by 30 inches to the walls. For this analysis, the chart displays what was being looked for. In the distribution chart in Figure

3.10 it can be seen that there was the possibility of a one by one room mode at this frequency.

The peaks at 68 Hz reach about 4 to 5 dB change. The natural peaks in the narrow band frequency reach much higher than this value. This peak was not significant enough to eliminate in the system and the frequency is not narrow enough to isolate. The possible presence of this room mode does not have a significant effect on the sound data. The remaining room mode predictions do not appear to have sound level distributions to match.

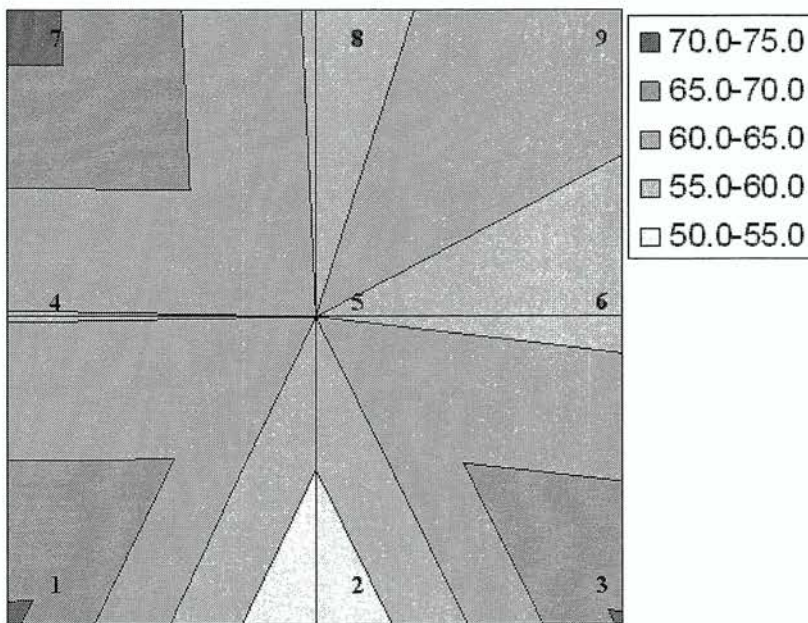


**Figure 3.10** Sound level distribution chart

### 3.4.2 Duct Modes

One of the main reasons for having duct measurements at multiple locations was to analyze the modes in the duct. Although the noise level in the duct was not as important as the noise level in the room, the duct is still part of the room. Modes that resonate within the duct will likewise transmit into the measurement room.

The duct modes were estimated in the same way as the room modes using equation 3-1. Given the dimensions of the duct, there were only a few frequencies that were likely to have duct modes. These predictions are shown in Table 3.6.

**Table 3.6** Duct Mode Predictions

X	Y	Z	Freq
0	0	1	26.79
0	1	0	140.67
0	1	1	143.20

The narrow band sound pressure levels are shown in Figure 3.11. These are the sound averages of 5 locations along the duct and not all 7. To identify the duct modes the sound pressure levels are observed along the cross section of the duct.

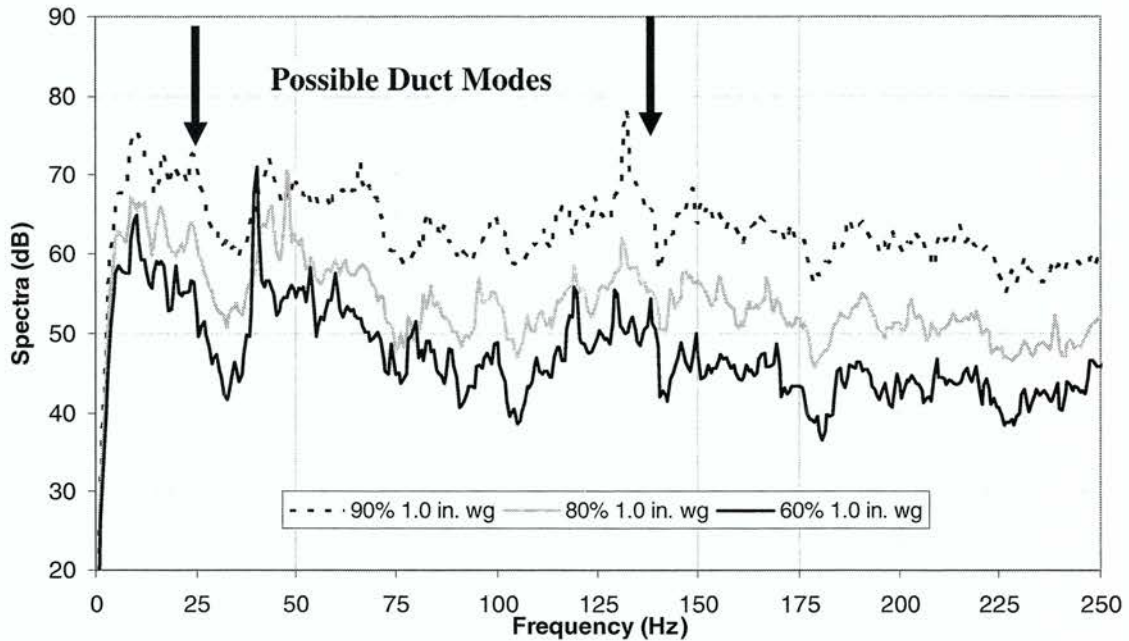


**Figure 3.11** Average Discrete Frequency Spectra in the Duct, Configuration 1, 0-Duct Diameters,  $\Delta P= 1.0$  inch

These frequencies were analyzed using similar methodology as used in the room mode analysis. There were three axes that can be observed using the duct sound pressure measurements. These peaks did not correspond to the mode predictions in the sound level distribution analysis.

Looking at both the room and duct narrow band frequency, sharp peaks can be seen. These peaks were not consistent between each operating point and are therefore not room or duct modes. These were likely caused by aerodynamic disturbances. The purpose of this facility was to measure the effects of aerodynamic disturbances on the sound levels so these peaks should be recorded.

## Chapter 4 Preliminary Sound Results

From Chapter 3 it can be seen that the sound results were obtained with good repeatability,  $\pm 1$ dB. This section will focus on the sound results that are obtained and the methods of interpreting the data meaningfully. More work must be done with the data for it to be adequately analyzed and interpreted.

All the sound data was analyzed compared to a “baseline” condition, and this chapter will cover how the baseline condition was determined and used. This chapter will also cover a series of methods to analyze the data. This will include comparing the sound levels with different fan discharge conditions. The change of sound levels at different operating points will also be looked at. The velocity distributions will also be displayed from the airflow station. These are all methods that may be useful in analyzing the sound data in the future.

### **4.1 Baseline Sound level**

The sound results were analyzed in terms of the change in sound level compared to a baseline. The base line that was used for comparison was the first configuration with one duct diameter ( $L/D=1$ ) between the fan and transition duct. This was used because it was considered the “optimum” outlet discharge condition by ASHRAE standards. As will be seen later in the paper this is not always the case.

Figure 4.1 displays the one-third octave band levels at this “optimum” configuration. The plots were grouped by fan pressure drop. The data in Figure 4.1 shows that at a constant pressure drop the noise increases as the %WOF curve increases. This was because there was more air flow, rpm and higher aerodynamic disturbances. It should be noted that in the

baseline system the 31.5 Hz one-third octave band drops considerably for many of the operating conditions. For the 1.0 inch pressure drop measurements, the 31.5 Hz one-third octave band drops around 10dB, for the 4.0 inch pressure drop measurements it drops 5 to 8 dB. At 2.5 inch pressure drops, the sound at the 31.5 Hz band was less than 5 dB.

## **4.2 Configuration Change**

It has been found that one of the best ways to examine and interpret the sound pressure level data was by looking at either each configuration separately, or by looking at all configurations a single distance between the fan outlet and transition ( $L/D=1$ ). The changing configuration demonstrates the differences that the configuration induces on the system. In some duct diameter distances, this effect was obvious and in others the effect can not be discerned.

The method of comparing these configurations was by looking at the differences between the sound levels of each configuration and the baseline configuration. This method was done at each of the one-third octave bands. Figure 4.2 shows the difference between the base line configuration and Configuration 4. This sound level data was taken with the fan running at 80% wide open flow and at 1.0 inch pressure drop. In this way, the data can be interpreted in levels of dB change. The highest dB change between the “optimum” and “worst” configuration at this operating condition is 11 dB. At the high octave bands the values become the same, meaning there is no effect on the sound levels of the system.

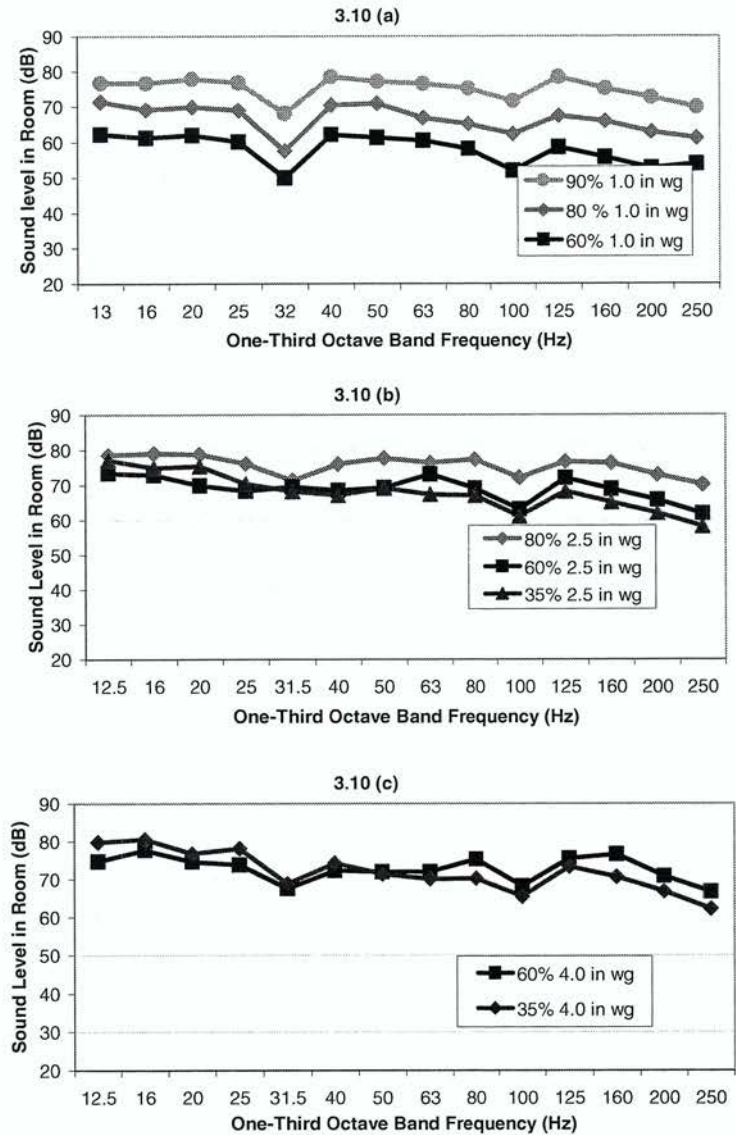


**Figure 4.1** Average one-third octave band sound levels in dB at configuration 1, 1 duct diameter. 3.10 (a) is the operating points at 1.0 inch water pressure drop. 3.10 (b) is the operating points at 2.5 inch water pressure drop. 3.10 (c) is the operating points at 4.0 inch water pressure drop.

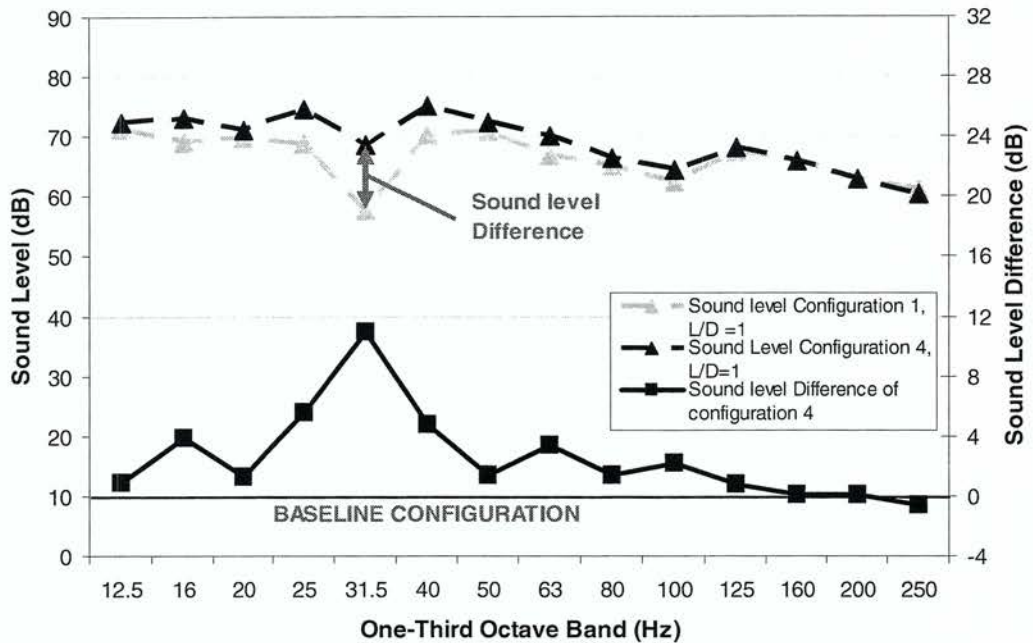


**Figure 4.2** Sound Level Differences

Figure 4.3 shows the sound level differences between the configurations and the “baseline” of all the operating points, one duct diameter away from the fan inlet ( $D/L=1$ ). Configuration 1 is the base line and is the zero line on all of the graphs. It is clear that at most of the operating points the noise increases as the configurations change. There were two exceptions to this. One is configuration 4 at 90% 1.0 inches; this configuration was quieter than the configuration 3 and at 35% 4.0 inches of water pressure drop configuration 4 was likewise quieter than configuration 3 at the lower one third octave bands. This was odd because the configuration 4 should have the most aerodynamic disturbances at the outlet of the fan and at the interaction with the elbow. The operating point at 90% and 1.0 inch water pressure drop had a very high flow rate; thus, the configuration effect on an already turbulent system may not have as much of an effect.

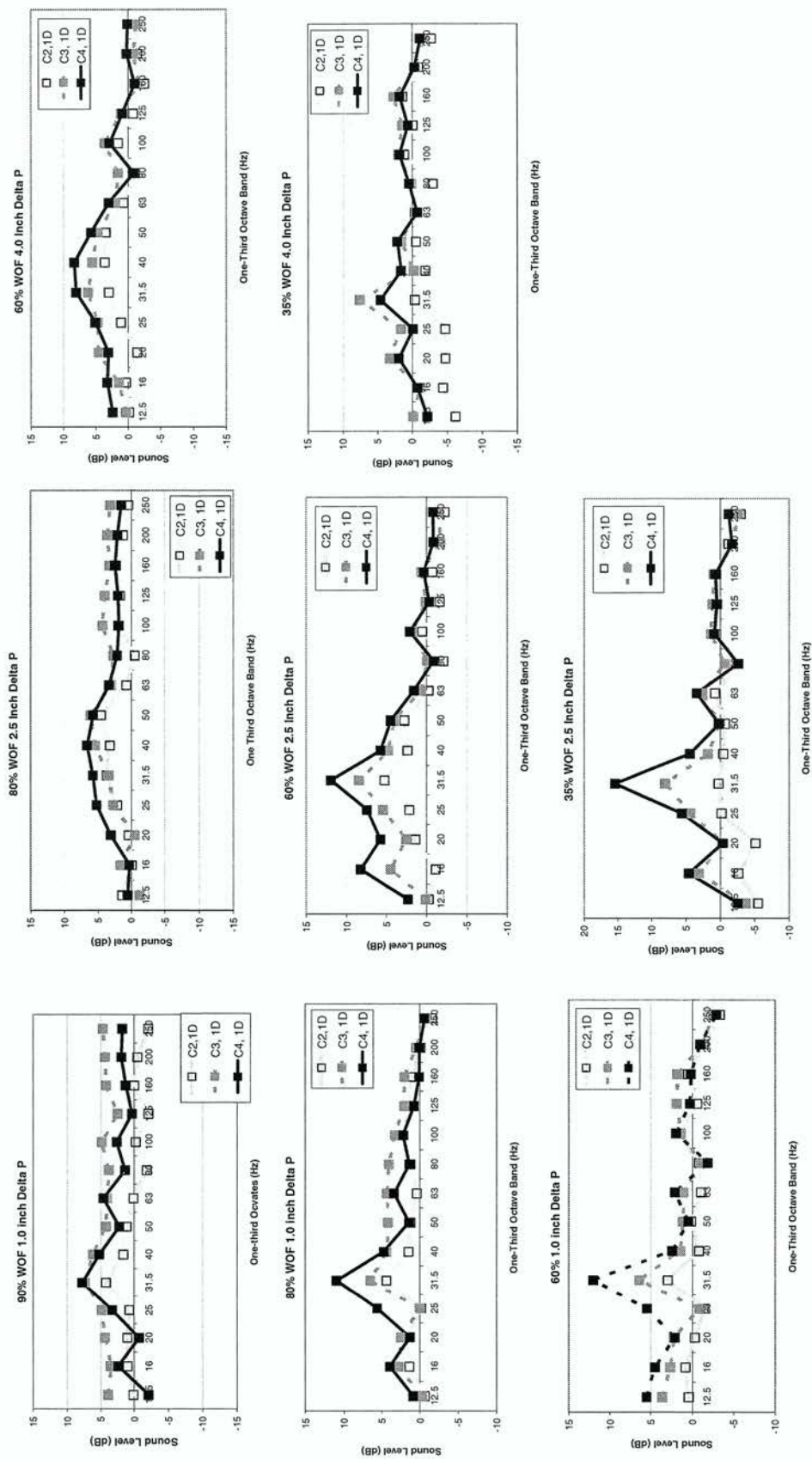


**Figure 4.3** Four discharge configurations at the eight different operating points. The first column of plots are the 1.0 inch pressure drop sound level differences (90%, 80%, and 60% WOF). The second is the 2.5 inch pressure drop sound level differences (80%, 60%, 35%). The third column is the 4.0 inch pressure drop sound level differences (60%, 35%)

At some one-third octave bands, the configuration 4 was quieter than configuration 2. The other operating point where the configurations were not so strong was at 35% and 4.0 inch pressure drop. At this operating point, configuration 2 has a negative value; meaning that configuration 2 was quieter than the “baseline” configuration. There were other scattered one-third octave bands where the sound level did not increase with configuration, but these were scattered and do not seem to be consistent throughout the whole operating point.

The largest changes that were seen in the sound levels happen at low frequencies, generally below the 80 Hz one-third octave band. This low frequency change indicates that the aerodynamic disturbances did adversely affect the low frequency ranges.

### **4.3 *Narrow Band Data***

The one-third octave bands were analyzed for good reference however, the narrow band data must be looked at in order to fully understand what was happening in the frequency spectra. With the narrow band data, the peaks at specific frequencies can be analyzed. The one-third octave band data can be used as a difference in dB to the baseline, the narrow band does not use the baseline for this. It was more useful to compare the sound levels directly, and in this way, the data can be taken at different frequency resolutions and still be compared to each other.

There were very large sound level increases in 6 of the 8 operating conditions, at the 31.5 Hz one-third Octave band. Many of these operating conditions are the same in that there was a decrease at this octave band in the baseline case. In two of these conditions there was not a drop at the one-third octave band. The 60% and 35% at 2.5 inch pressure drop

operating conditions both have large increases at the 31.5 Hz one-third octave band. They both also have an increase at the 16 Hz one-third octave band. In Figure 4.4, the narrow band frequency of all operating conditions at 2.5 inch pressure drop can be seen for configuration 4, 1 duct diameter. By looking at the narrow band sound pressure level data, it can be seen that there was a large tone at 15.5 Hz and at 30.3 Hz in the two operating conditions. These tones explain the sharp increase at those one-third octave bands. However, it was important that these peaks are not entirely what were causing the increase in sound levels.

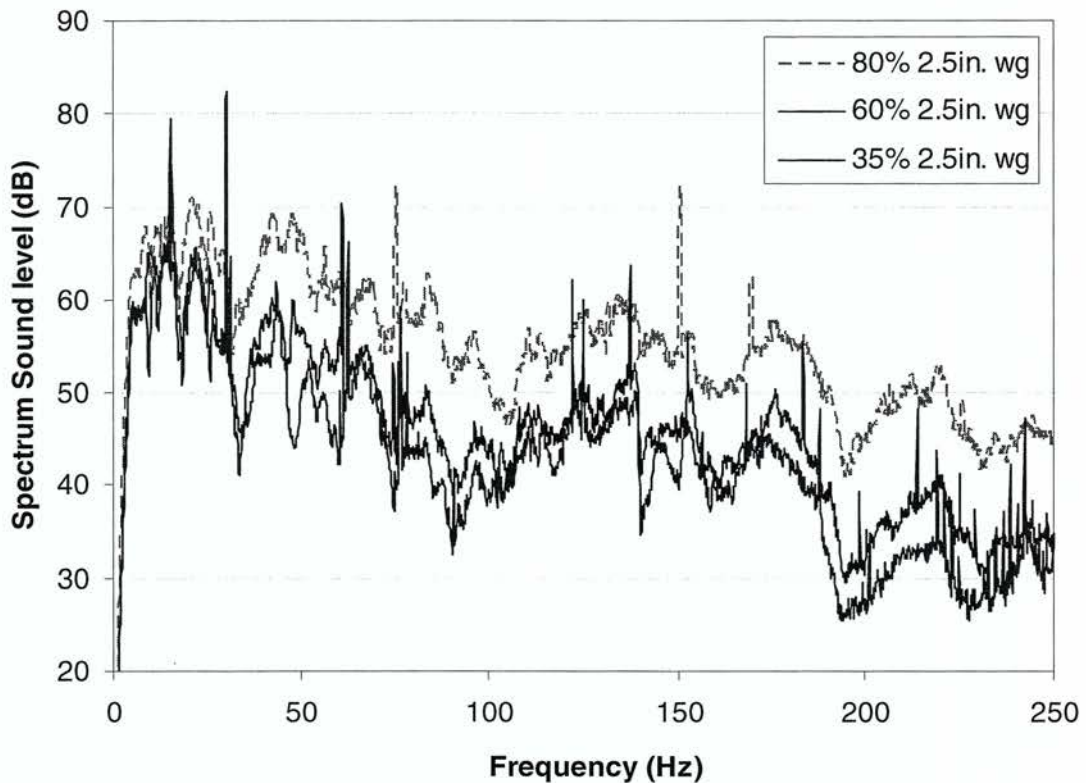


**Figure 4.4** Narrow Band Sound Level Data Configuration 4, one duct diameter to the elbow (L/D=1)

Figure 4.5 shows the comparison of two configurations at one duct diameter between the outlet of the fan and the elbow ( $L/D=1$ ). The frequency was only taken out to 100 Hz. As stated earlier the major effects happen at the low frequencies and the high resolution makes it difficult to distinguish the narrow band sound levels. Here, it can be seen that the peaks in the data have increased; however, it can also be seen that the rest of the sound level was higher. Thus, the peaks increase with the rest of the sound level. More work must be done to determine if these peaks need to be isolated or if they should be measured with the rest of the sound data.

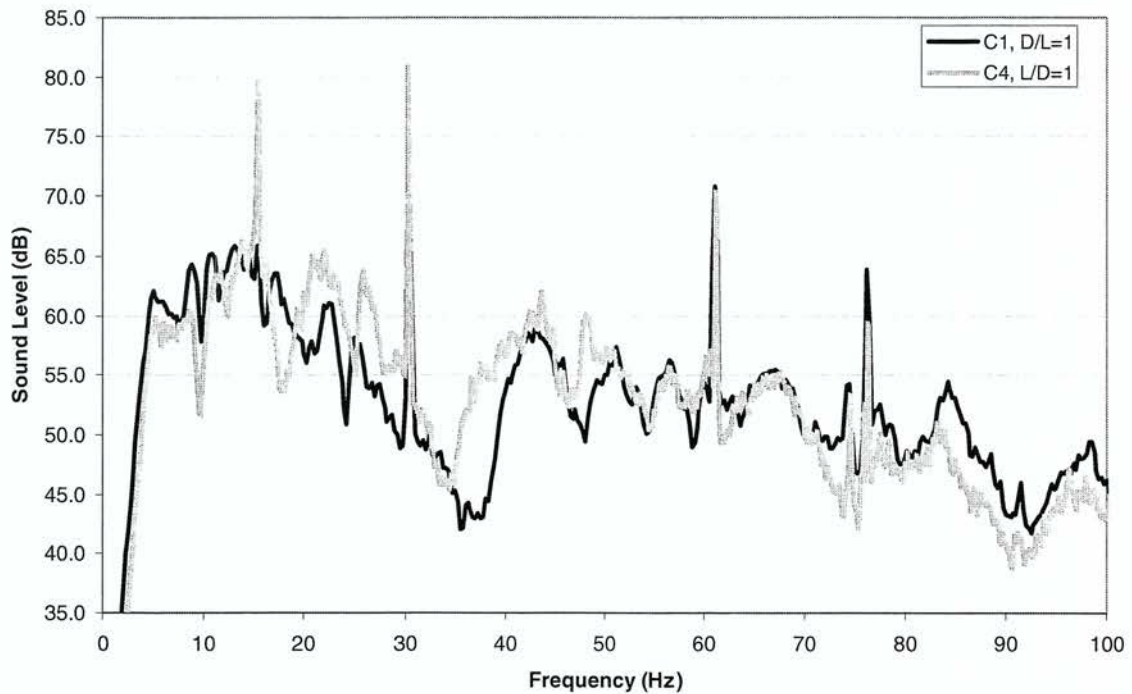


**Figure 4.5** Narrow band sound level data of configuration 1 and configuration 4.

#### **4.4 Difference of Operating Points**

The main focus of this report was the effect that discharge configuration has on the downstream duct rumble noise. However, the effects of the change in operating point are important. The reason to run the fan at multiple operating conditions was to populate the fan curve enough to make the data useful in practice. In many situations, in commercial HVAC systems, if the needed airflow rate was not achieved, then the fan speed is increased until the flow rate is reached. This practice means that many systems are not necessarily operating at one of the operating points that are set here in this study. Having eight operating points could give an indication of what happens as the fan moves along a load curve. More work must be done with this to accurately analyze the measurement of the effects at different operating points.

The change between the baseline and configuration 2 at one duct diameter is shown in Figure 4.6. The noise increases with fan speed and increases with airflow rate, except at the high pressure drop of 4.0 inches of water. In many cases, the sound change increases with flow rate, and in most cases the sound level change also increases on the load curve as flow rate and pressure drop increases, which corresponds to an increased fan speed. However, in a few cases, notable the 60% load curves in Figure 4.6, the noise decreases at the higher fan speeds. In this case, the data is from the 80 Hz one-third octave band. These results suggest that the increased noise was caused by higher aerodynamic disturbances. This was a trend that was observed, however there are exceptions to this trend at several octave bands that would indicate that it needs to be explored before making a conclusion.

Figure 4.7 shows the change in horsepower that the VFD draws at each operating point on the fan curve. From this figure, it can be seen that there was very little

correlation between the change in horsepower and the change in sound. What this meant was that change in sound again comes from the turbulence and the airflow disruptions. The motor operates at relatively the same power.

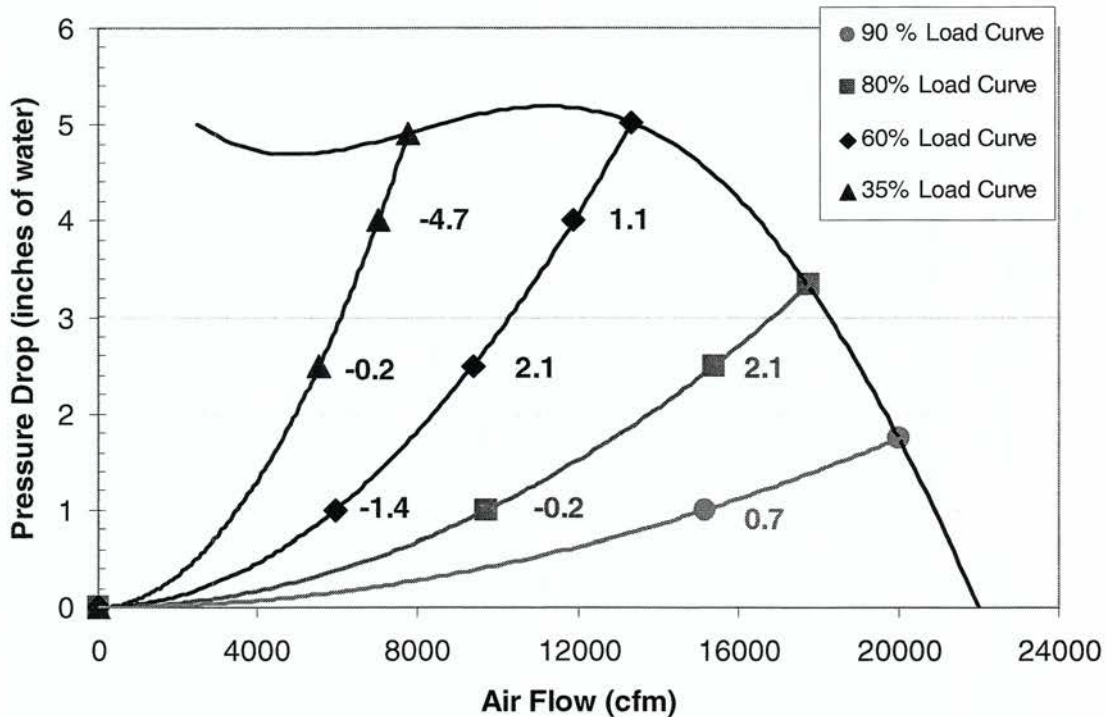


**Figure 4.6** Room Sound levels difference in (dB) relative to configuration 1 and L/D=1 duct diameter. 80 Hz one-third Octave band. Configuration 2, L/D = 1 duct diameter.

## 4.5 Velocity Profiles

The velocity profiles were not precise results, but they give an insight the air flow in the duct work. The velocity profile can be measured at the airflow station, and than used to determine if the flow had become laminar or not by the time it reached the airflow station. In addition, it can also be determined if the airflow is balanced at the inlet. If the flow has very large values on one side and very low on the other, then the air into the fan may on be even

on either side. This velocity profile allowed checking if an inlet baffle was necessary. The inlet baffle was discussed in chapter 2.

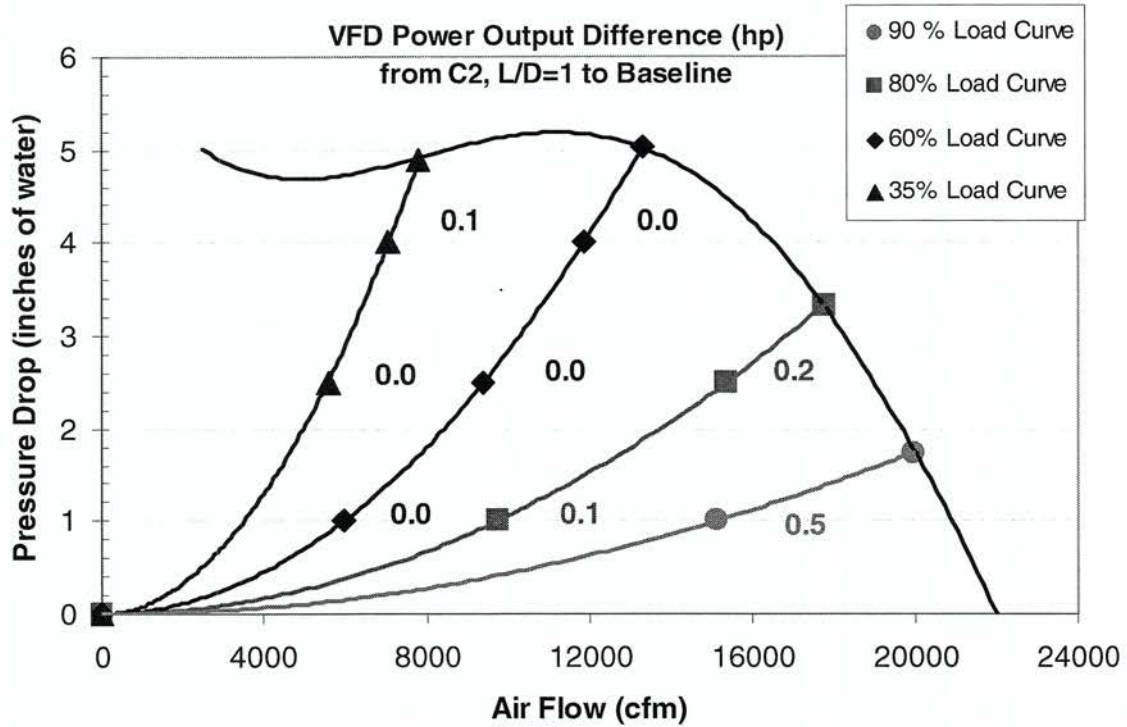


**Figure 4.7** Power output difference of the VFD (hp)

Four configurations are shown in Figures 4.8 and 4.9; both are at the same operating point, 90% WOF load curve at 1.0 inch pressure drop, and the same distance from the fan to the elbow L/D. Figure 4.8 shows the comparison of the configuration 1, “baseline” and configuration 2. Figure 4.9 shows the comparison of configuration 3 and configuration 4. In these figures the external limits of the graphs were not at the walls of the duct, as there was no way of measuring these points. In addition, the distribution of each of these points matches the distribution in Figure 2.15. The graphs in Figures 4.8 and 4.9 are not to geometric scale.

It can be seen from these Figures 4.8 and 4.9 that the velocity profile changes as the configuration changes. The operating point that was displayed was consistent with the velocity distributions of the remaining operating points.

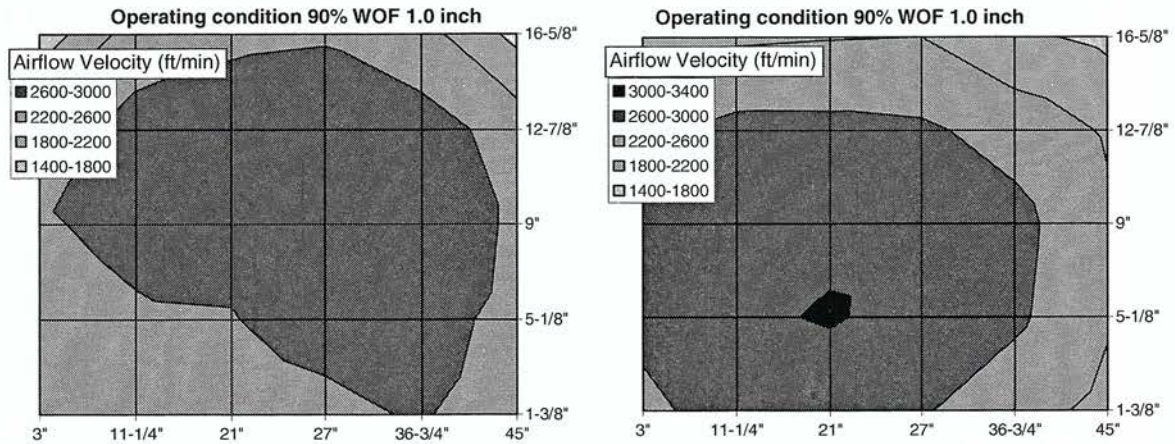


**Figure 4.8** Velocity profile of configuration 1 and configuration 2, at 90%WOF and 1.0 inch pressure drop, with one duct diameter between the fan and elbow.

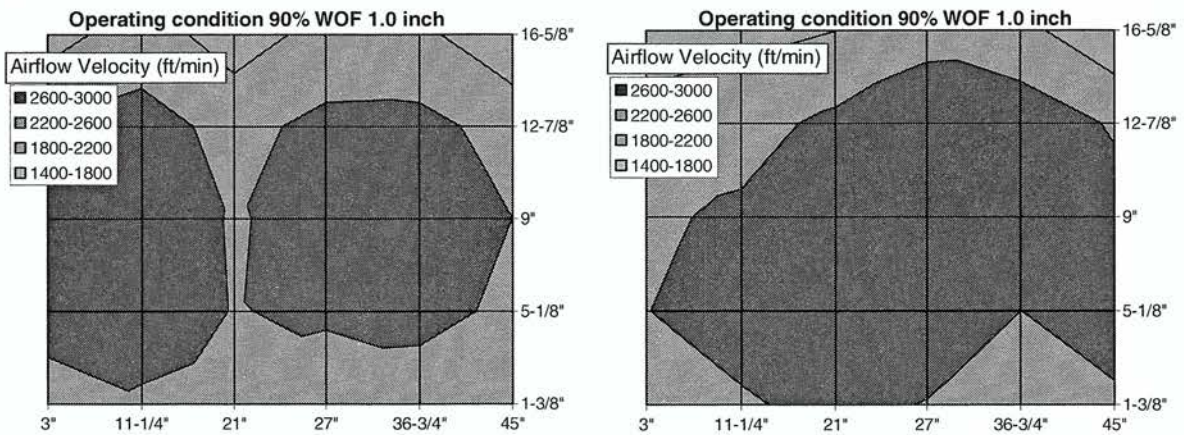


**Figure 4.9** Velocity profile of configuration 3 and configuration 4, at 90%WOF and 1.0 inch pressure drop, with one duct diameter between the fan and elbow.

## Chapter 5 Summary and Conclusions

### 5.1 Summary

The system in this study was created to accurately measure the effects that aerodynamic disturbance caused by fan discharge conditions has on downstream rumble noise production. Aerodynamic disturbances are the most common cause of low-frequency duct-rumble noise. In this case, duct-rumble noise is defined as sound below 250 Hz. The system was flexible enough to handle a total of four different fan discharge configurations and four different duct lengths between the fan outlet and the HVAC ducting inlet. The fan can be operated under any number of operating conditions, but eight operating conditions had been selected for this study to gauge the effect each configuration has on rumble noise. These test variables gave a total matrix of 112 test conditions.

The HVAC system was designed to create an easily measured value of sound pressure level. The HVAC system runs through three rooms: a fan room, a measurement room and an outlet room. The fan room has a mounting base and a rising base that allows the easy change from one configuration to another. The fan room also had an inlet restriction that allows the control of the %WOF (percent wide open flow) load on the fan. This inlet restriction, along with the change in fan speeds allows for the setting of the various operating points. The operating points selected for this study were:

- One operating point at 1.0 inch water gage pressure drop representing the 90% wide open flow load curve
- Two operating points at 1.0 and 2.5 inch water gage pressure drop representing the 80% wide open flow load curve

- Three operating points at 1.0, 2.5 and 4.0 inch water gage pressure drop representing the 60% wide open flow load curve
- Two operating points at 2.5 and 4.0 inch water gage pressure drop representing the 35% wide open flow curve.

The measurement room was acoustically isolated from the rest of the facility to ensure good measurements. The noise reduction between the fan and measurement room at least 13 dB at all frequencies. The duct work that was in the fan room was enclosed in medium density fiberboard and insulation to prevent break in noise from the fan and motor assembly. The duct discharges into an outlet room through an outlet plenum. The outlet plenum prevents noise from outlet room back into the duct system.

There were several measurements that were made on this system. The sound pressure level measurements were the focus of this study. The sound was recorded in nine locations throughout the room and at three different heights, 36", 56" and 81" above the floor. The nine locations were spaced in a 3 by 3 grid with the rows spaced 30" apart and the columns were spaced 40" apart. There were seven sound pressure level locations that were measured in the duct and at two joints. The primary function of the in duct measurements was to identify modes in the ductwork. There were six microphone locations along a duct joint that is 53" away from the outlet room wall, and the seventh microphone location was at a corner of the duct work just as it entered the measurement room. These locations gave good duct mode indicators for all three axes of the duct. The microphones record the one-third octave band sound pressure levels from 12.5 to 20,000. These were averaged over 30 seconds. A narrow band frequency is recorded up to 800 Hz, at 100 averages.

An airflow station was placed 6.4 duct diameters (16'-6") downstream from the transition exit and 1.9 (5') duct diameters upstream from the outlet plenum. This airflow station consisted of a six pitot tube traverse grid connected to rigid cross bars. These cross bars can be raised and lowered to five notched locations, allowing for 30 pressure measurement locations within the duct. This traverse gave the velocity pressure, which is used to calculate the velocity distribution and the average cubic feet per minute. This station can also measure the pressure drop between the airflow station and the fan room by means of a pressure tap that is located in the fan room. This pressure measurement was used to estimate the pressure drop across the fan, but it was considered too unreliable to set the operating conditions. The pressure drop measurement was recorded, but the fan laws and the fan curve were used to set the operating conditions.

The system was tested for repeatability for the sound measurements. The system was tested three times, and an average was taken of the three tests. The repeatability was proved to be less than  $\pm 1$  dB of the average for any given one third octave band.

The vibration of the fan and motor assembly were recorded to check any effect they have on the sound data. The vibrations were taken at two locations. One was on the fan along a steel plate that supports the fan bearings; the other was on the motor base. These measurements recorded a velocity time signal and a discrete frequency spectrum. The time signal was eight seconds and the discrete frequency spectrum recorded 100 averages.

## **5.2 Conclusions**

The test facility can be used to accurately measure sound pressure levels and operating conditions of a fan and was flexible enough to study many configurations. The

system isolates the noise in the measurement room. The system can create four different fan discharge orientations and four duct lengths in between the fan and the elbow. The test system can measure the effects of the aerodynamic disturbances that the fan discharge conditions create. The system can accurately measure the one-third octave band level to within  $\pm 1$ dB. The air flow can be accurately measured to within  $\pm 1.5\%$ .

The vibration of the fan and motor assembly was of great concern. The ASHRAE RFP called for a tri-axial peak velocity no greater than 0.15 inches per second in any direction. The velocities that were measured were well above this limit by an order of 10 to 60. The impact on the sound data needed to be analyzed; at frequency of vibrations, many of the peaks occurred at the fan rpm frequency. However, the sound peaks and the vibration peaks did not necessarily match. Many of the sound peaks occur at the 4<sup>th</sup> harmonic. This information suggests that the cause of the noise was the aerodynamic interference that was caused by the fan cage supports, four of which are located at the inlet of the fan. Given that this was an integral part of the fan, these aerodynamic disturbances must also be measured.

System modes may occur in the room or in the duct. The room was small and selected to limit the number of modes at low frequencies. The room and duct modes were estimated, and then these estimates were compared to the sound level distribution in the room. These distributions indicated that there were a few duct and room modes at 100 Hz and 68 Hz that needed to be addressed. The narrow band frequency was then analyzed at the frequencies, and it was seen that these modes did not have a large impact on the sound pressure level so they were not isolated.

The preliminary sound results show that when the fan was directly next to the inlet of the duct system there was no clear trend as to what was louder or quieter. However, as the

fan was moved at least one duct diameter away, the trend appears that the noise level increases as the configuration changes towards more aerodynamic disturbances, this was not the case at some operating conditions, 35%, and 4.0 inch pressure drop in particular. The results also point to a diminishing return as the fan was moved farther away from the inlet of the duct system.

### **5.3 Recommendations for Future Study**

The analysis section of this study requires more work to turn the data that has been collected into a practical and useful format. The effects of orientation on the system can be seen, as can the effects of duct distance between the fan and the elbow. However, the analysis must go more in depth to fully understand the effects of the aerodynamic turbulence. Trends could be seen along the fan curve; however, more work can be done, particularly with the brake horse power of the fan and motor. With the data that has been obtained, the fan curve could be populated and used to predict the sound level effects of moving along load curves or pressure curves.

This facility could be used for quite a number of additional projects. It was most suited for measuring the fan noise of different fan sizes and fan designs. Each fan will have different aerodynamic disturbances within it. This facility was also flexible enough to change aspects of the system. The volume damper could be placed at the outlet instead of the inlet. The flexibility in the inlet could also more accurately define the effects of aerodynamic disturbance with respect to the location on the fan curve. During this study, there has been a lot of controversy as to how duct rumble was defined and here in it was assumed that duct rumble was the sound levels below the 250 Hz octave band. However, it could be argued

that the cause of duct rumble was the time dependence of the sound level. This test facility can record time dependent data along with simple sound recordings to compare the perception of what was duct rumble. The time varying data could be used to redefine what causes duct rumble.

## References

ASHRAE (2004). ASHRAE Handbook-2004 ASHRAE systems and Equipment, American Society of Heating, Refrigeration and Air-conditioning Engineers Inc.

ASHRAE, (2005). ASHRAE Handbook-2005 Fundamentals, American Society of Heating, Refrigeration and Air-conditioning Engineers Inc.

ASHRAE, (2003) ASHRAE Handbook-1987 HVAC systems and applications, American Society of Heating, Refrigeration and Air-conditioning Engineers Inc.

ASHRAE, (1999) ASHRAE Standard 51-1999- Laboratory Methods of Testing Fans for Aerodynamic Performance Rating, American Society of Heating, Refrigeration and Air-conditioning Engineers Inc.

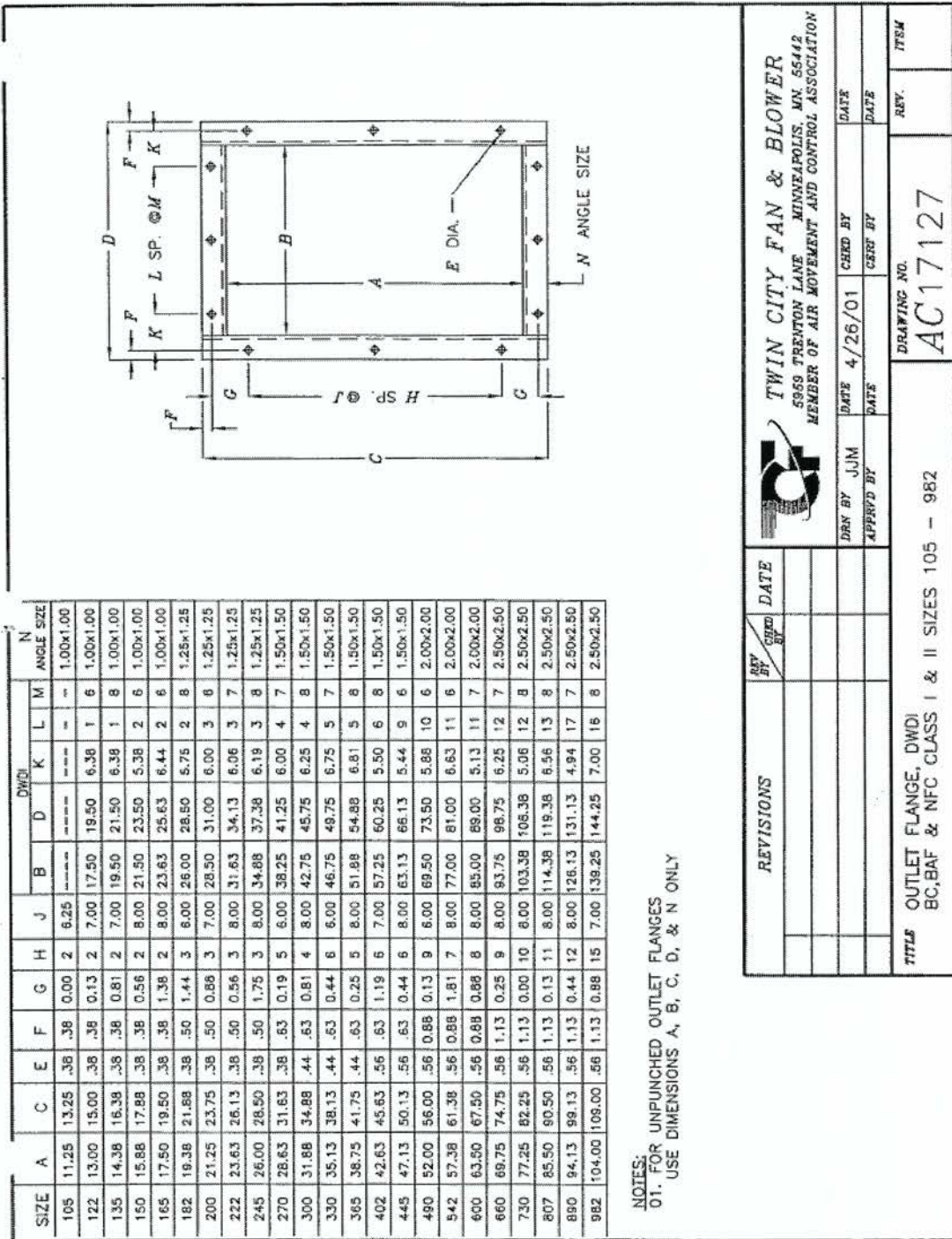
Bies and Hansen (2002) "Engineering Noise Control Theory and Practice", New York, NY: Spon Press. p. 227

Mark Schaffer P.E., Technical Committee Member, Schaffer Acoustics, Personal Interview, Nov 18, 2004.

Steve Wise, Technical Committee Member, Personal Interview, June, 2005.

Kim Osborne, Technical Committee Member, CES Laboratory Manager, Telephone Interview, September, 2005.

# Appendix – Twin Cities Fan Information



NOTES:  
 01. FOR UNPUNCHED OUTLET FLANGES  
 USE DIMENSIONS A, B, C, D, & N ONLY

Figure A. 1 Twin Cities Fan Flange Dimensions



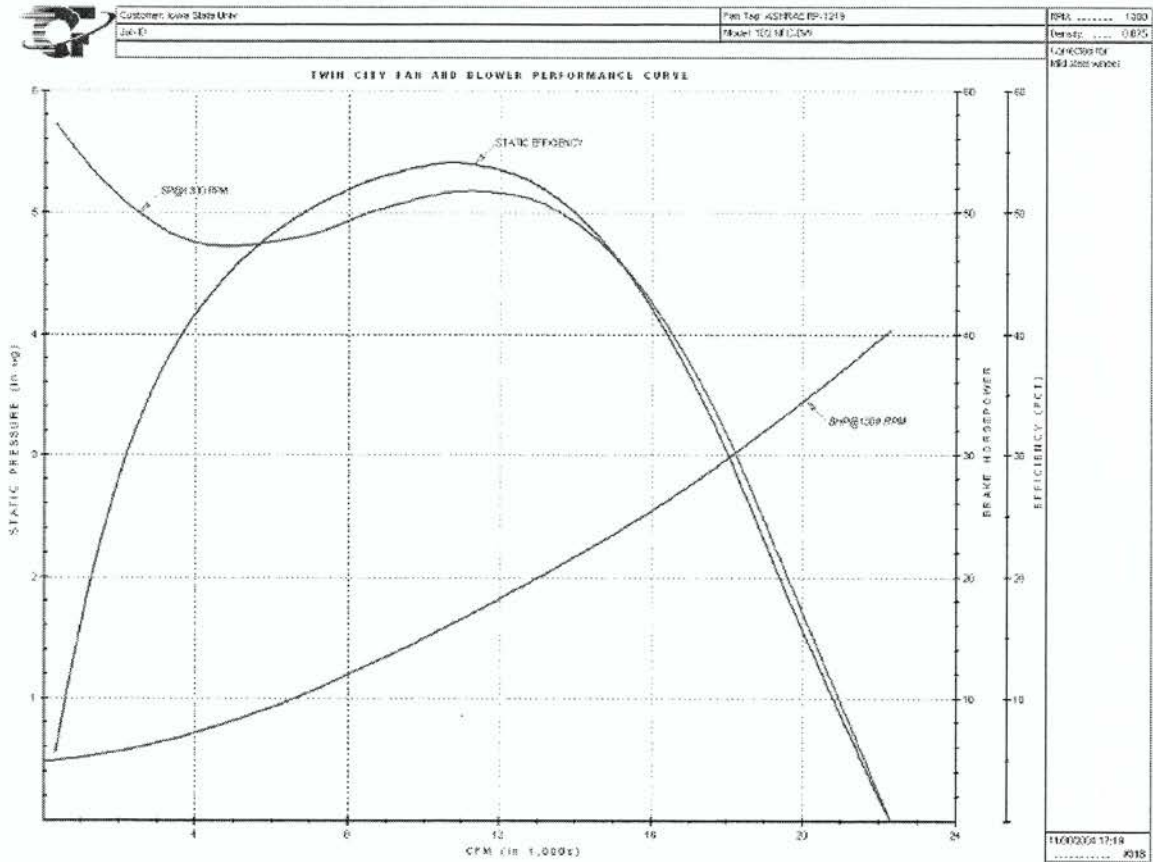


**Figure A. 3 Twin City Fan Curve**